Natural Hazards (2024) 120:5333–5368
https://doi.org/10.1007/s11069-023-06398-9

ORIGINAL PAPER

Mapping of flood hazard induced by land subsidence in Semarang City, Indonesia, using hydraulic and spatial models

B. D. Yuwono[1] · H. Z. Abidin[2] · Poerbandono[3] · H. Andreas[2] · A. S. P. Pratama[5] · F. Gradiyanto[4]

Received: 16 February 2023 / Accepted: 28 December 2023 / Published online: 7 February 2024

Abstract

Frequent floodings in Semarang City have generated increasing damages and losses in property and life quality. The cause of flooding is related to the coupled impacts of land subsidence, hydraulics hazards along with poor drainage and water retention systems. This paper studies the most recent flooding hazards caused by hydrological origins (i.e., river discharge, tidal) and land subsidence. In the study, riverine origin of flooding is simulated with the help of HEC-RAS 2D, while the tidal origin is simulated to high highest water level. However, due to the absence of the most recent topographic data, the role of land subsidence is measured by estimating the vertical changes of digital elevation model taken from Sentinel 1A. Flooding extent, in terms of depth and coverage, is verified based on satellite imagery Sentinel-2 which is cloud-processed using Google Earth Engine (GEE) and field survey. Fluvial flood is simulated with several boundary condition scenarios using combinations of 5-, 25-, or 50-year return periods of flood which is integrated with mean sea level (MSL) or high highest water level (HHWL) tides. Those boundary conditions are then incorporated into different terrains, namely LiDAR, DEMNAS, and TerraSAR DEM, to see how different digital elevation models (DEMs) can impact model sensitivity. By overlaying model outputs and land cover map, it can be concluded that settlements and water bodies are among the most potentially affected areas, covering up to 17 km^2. This study is expected to help policymakers make a primary assessment of combined tidal and fluvial flood hazard through mitigation and adaptation measures.

✉ B. D. Yuwono
bdyuwono92@gmail.com

[1] Doctoral Program, Geodesy and Geomatics Engineering, Faculty of Earth Sciences and Technology, Bandung Institute of Technology, Jalan Ganesha 10, Bandung 40132, Indonesia

[2] Geodesy and Geomatics Engineering, Faculty of Earth Sciences and Technology, Bandung Institute of Technology, Jalan Ganesha 10, Bandung 40132, Indonesia

[3] Hydrography Research Group, Geodesy and Geomatics Engineering, Faculty of Earth Sciences and Technology, Bandung Institute of Technology, Jalan Ganesha 10, Bandung 40132, Indonesia

[4] Civil Engineering Department, Engineering Faculty, Diponegoro University, Tembalang, Semarang 50275, Indonesia

[5] Master Program, Geodesy and Geomatics Engineering, Faculty of Earth Sciences and Technology, Bandung Institute Technology, Jalan Ganesha 10, Bandung 40132, Indonesia

Keywords Hazard · Land subsidence · Digital elevation model · Fluvial flood · Tidal flood

1 Introduction

1.1 Background and rationale

Semarang City, the capital of Central Java Province, Indonesia, has been suffering from episodic flooding that generates increasing annual losses. It was reported that the economic loss of approximately 20 years under business as usual scenario (BAU) amounts to 79 trillion IDR (present value), which translates into about 2% of GRDP per year (Mahya et al. 2021). Another report noted a severe flood happened in early 1990, due to overflow of Garang river and other flowing rivers through the City of Semarang. It resulted in 47 deaths and losses counting to 8.5 billion IDR (at that time) (Dewi 2007).

Flooding in Semarang is getting worse under the influence of land subsidence (Yuwono et al. 2016; Abidin et al. 2012; Abidin et al. 2013). The phenomenon of land subsidence in Semarang has been investigated through a combination of methods, including levelling surveys (Marfai and King 2007; Murdohardono et al. 2007), GPS surveys (Abidin et al. 2013; Andreas 2019), DInSAR (Yastika et al. 2019; Chaussard et al. 2013; Lubis et al. 2011; Kuehn et al. 2010), microgravity (Supriyadi 2008), and geometric-historic approaches (Abidin et al. 2015). In general, land subsidence in Semarang City has a spatial and temporal variation with typical rates of about 3–0 cm year^{-1}.

Research on land subsidence in Semarang is urgently required due to adaption and mitigation measures for flooding. Floods triggered by land subsidence resulted in significant catastrophic damage such as economic losses (Kurniawati et al. 2020; van de Haterd et al. 2021), infrastructure damage (Putra et al. 2020), land value change (Amar et al. 2020; Utami and Marzuki 2020), and environmental damage (Marfai 2014). The community's socio-economic activities are also impacted by the inundation depth and duration, causing increased population relocation, deteriorating public health, disruption of livelihood activities, and unpredictable income levels (Pratikno and Handayani 2014). One flood with such impacts was flood 2020, which was found on Terboyo arterial road and the North Semarang area (Fig. 1).

According to Merz (2010), flood risk mapping is an essential element of flood risk management and risk communication. It is used to determine flood-prone locations and enhance flood risk management and catastrophe readiness. Flood hazard assessments and maps often examine the anticipated extent and depth of flooding in a specific place, depending on various scenarios (e.g., 100-year events, 50-year events, etc.). Flood hazard maps are intended to make the public, local governments, and other organizations more aware of the likelihood of flooding. Additionally, they advise those who live and work in flood-prone locations to learn more about their region's flood risk and take the necessary precautions (Uddin and Matin 2021).

1.2 Previous flooding studies

The mapping of flood hazards has been conducted by The Disaster Management Capacity of the National Agency for Disaster Management (BNPB) using topographic index (BNPB 2016). The calculations heavily depend on the resolution of the Digital Elevation

Fig. 1 Flood extent induced by land subsidence in North Semarang on 19 Dec 2020. **a** Arterial road Terboyo. **b** Inundation in Islamic Sultan Agung Hospital and c. The deteriorated environment in Tambak Lorok

Model (DEM) and slope. The generated flood maps cannot yet differentiate whether the floods are caused by river overflow or tidal flooding. Additionally, the recent changes in topographic surface dynamics, where the Semarang region is experiencing land subsidence, have not been considered in the modelling.

Tidal and fluvial floods are two distinct types of flooding events that occur due to different causes. Tidal floods, also known as coastal or storm surges, result from the rise and fall of ocean tides combined with strong winds and storms (McInnes et al. 2003). These floods typically affect coastal areas and are influenced by factors such as lunar cycles and weather conditions. On the other hand, fluvial floods, often referred to as riverine floods, stem from the overflow of rivers and streams due to excessive rainfall or snowmelt. Fluvial floods are prevalent in inland regions and can be exacerbated by factors like topography and land use. Although tidal and fluvial floods differ in their sources and locations, both pose significant risks to human settlements and infrastructure. Tidal flooding has a significant contribution in causing inundation in Semarang (Marfai et al. 2008). Tidal flooding caused by high tides and land subsidence seriously threatens urban areas in Indonesia. Floods will overflow or overtop barriers like dikes, resulting in the land behind the dikes being inundated and prone to flooding. The low-lying areas of various cities in Indonesia, such as Semarang, often experience tidal floods (Kobayashi 2003). Several studies suggested that tidal flooding in Semarang is due to the combined influences of land subsidence and sea level rise. It was recorded that in May 2005, at least 14 sub-districts were inundated by tidal flooding with an inundation area of 2.6 ha (Ismanto et al. 2012). However, historically the worst tidal flood conditions occurred in 2013 which were triggered by high tides. As a result, six districts in Semarang were submerged with inundation heights reaching 1 m (Irawan et al. 2021). Handoyo et al. (2016) explained that the tidal flooding that occurred in the Semarang Utara district in 2014 covered 823.5 ha with Tanjung Mas as the most widely affected village. Figure 2 shows the map of study area that experienced flooding.

Most of the fluvial floods that happened in Semarang were triggered by high-intensity rainfall and the physical condition of Semarang city which is dominated by the lower areas in the north. Accumulated fluvial floods did not immediately flow into the sea and the areas became inundated instead (Wismarini and Ningsih 2010). These floods damaged hundreds of houses as well as several public facilities such as schools, mosques, and orphanages and killed six people (Waskitaningsih 2012).

DEM plays a crucial role in applying flood modeling as it provides essential topographic information needed for accurately simulating flood events. The DEM serves as a depiction terrain of the Earth's surface, enabling the generation of precise floodplain maps, identification of flow patterns, and computation of water depths for flood simulations. DEM data are fundamental for hydraulic models like HEC-RAS, which rely on accurate elevation information to simulate river flow, identify flow paths, and predict flood extents. Moore et al. (1991), Xu et al. (2021), Qin et al. (2018), and Han et al. (2020) highlighted the importance of DEM resolution in flood modelling. They emphasized that finer-resolution DEMs enable more accurate representation of floodplain topography, leading to improved flood predictions, better estimation of inundation extents, and more reliable flood hazard assessments.

In flood modelling, it is essential to correct DEM using land subsidence rate to accurately assess potential flood risk and inundation areas. DEM is used to depict the topography of the land, including the elevation of various points on the surface especially in areas that experience land subsidence. Land subsidence refers to the sinking or lowering

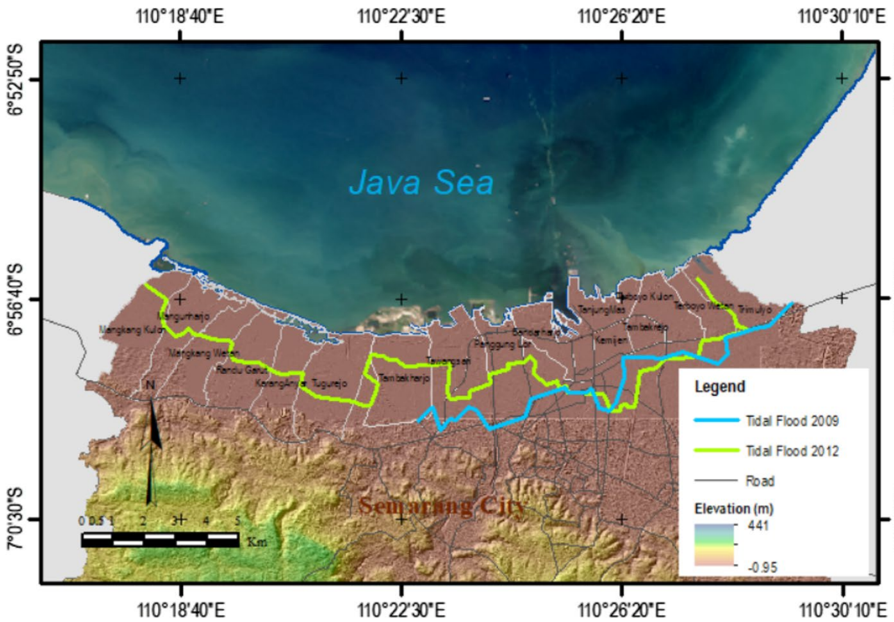

Fig. 2 Location map of the study area

of the Earth's surface, which can be caused by various factors such as groundwater extraction, natural geological processes, or human activities (Abidin et al. 2013). Irawan et al. (2021) used the major causes of inundation in coastal areas, i.e., extreme water levels and subsidence combined with sea level rise to obtain coastal flooding simulation. The DEM was used for boundary conditions using TerraSAR-X, which has a relative vertical accuracy of around 6 m and was corrected using the 2009 land subsidence rate. Zainuri et al. (2022) conducted an assessment of tidal flood inundation areas based on inundation height, rate of sea level rise, topographic height data, and land subsidence. DEM was obtained through a topographic survey, whereas land subsidence was processed using Sentinel-1 Synthetic Aperture Radar (SAR) image data with Single Band Algorithm (SBA) differential interferometry. Some of the methods used for assessing flood hazards include a spatial analysis mapping system with a GIS-raster system (Marfai and King 2008; Suhelmi et al. 2014) and physical modelling (Khattak et al. 2016). Marfai and King (2008) studied a GIS-raster system using a spatial analysis with neighborhood operation for tidal inundation mapping. However, spatial analysis with the neighborhood method does not consider hydrological analysis, i.e., discharge, stream, and flow velocity. Considering the physical modelling techniques, flood modelling is classified as 1D and 2D. Both the longitudinal and transverse directions of the river channel are taken into account by 2D hydrodynamic models for urban floods (Tarekegn et al. 2010). Two-dimensional hydraulic models are more commonly employed to solve unsteady flow problems that need more input data. Moreover, they can simulate the magnitude of the flooded area at different times (Horritt and Bates 2001). It has been discovered that integrating hydrological models with Geographic Information Systems (GIS) is beneficial in determining the geographical variability of flood hazards (Qi and Altinakar 2011).

Flood inundation analysis refers to the process of mapping and studying the scope and depth of flooding in a particular area. Two commonly utilized methods for analyzing flood inundation are HEC-RAS (Hydrologic Engineering Centers River Analysis System) and spatial analysis techniques. In the case of fluvial flooding caused by land subsidence in east Semarang, specifically in the Tenggang Watershed and Sringin Watershed, researchers utilized HEC-RAS to investigate this phenomenon (Pujiastuti et al. 2016; Aini and Filjanah 2020). The findings indicated that land subsidence contributed to a yearly increase of 1.39% in flood inundation. Additionally, spatial analysis techniques were employed to determine the extent of flooding (Marfai et al. 2008). The purpose of this study is to provide a case study on local spatial-scale flood hazards induced by land subsidence. The approaches proposed as a whole employ GIS, remote sensing, and hydraulic modelling to examine them in an integrated manner. Estimating maximal flood flows is crucial in calculating flood hazards (Q5, Q25, Q50). This study investigates how to evaluate the flood triggered by fluvial, tidal, and combined conditions. The study uses hydrology data from 6 rivers modelled with HEC-RAS 2D with 1m LiDAR high-resolution DEM with improving cross-section field data. The suggested procedures seek to identify flood intensity, depth inundation, the model area's sensitivity, and flood hazard level. Information on the characteristics and extent of the damage can be useful to predict future impact typology because impact types and severity within the flooded area can vary depending on factors like flood water depth, velocity, land cover type exposed, and others. Types of flood impacts, their locations and the severity of the impacts can be determined by tracking the spatial distribution of these impacts. Having said that, hopefully it will provide government officials as well as related stakeholders with an important reference for development planning, disaster prevention, and disaster mitigation.

2 Study site

Semarang is the capital of Central Java province, located at 6°58′ S and 110°25′ E on the northern coast of Java (see Fig. 2). It has a coverage area of about 37,370 ha, a coastline length of 13.6 km, and a population of 1.81 million people with a growth rate of 1.57% per year (Yuwono et al. 2019). Semarang's northern area is dominated by diverse infrastructures such as airport and bus stations, as well as densely populated areas, ponds, and agricultural land. Meanwhile, the southern area is dominated by green areas, open spaces, and settlements (Setioko et al. 2013). The geological structure of Semarang City is formed by three lithological units: volcanic rocks of the Damar Formation located in the South-West, marine sediments in the North, and alluvial deposits, also in the North (Kuehn et al. 2010). The northern part of the city is a coastal plain while the southern part is higher ground. The elevation level of this city varies from about 0–453 m (Marfai and King 2007). There are several rivers indicated to experience fluvial flooding namely Bringin, Silandak, Siangker, Banjir Kanal Timur, Tenggang, and Babon River.

3 Methodology

The methodology adopted for the study is shown in Fig. 3. The first step is developing a terrain data set directly in HEC-RAS by using the ras mapper tool. All geometric and hydrological data are modelled and utilized, including historical flood events for model

Fig. 3 Flowchart of research methodology

validation and designed flood events. The LiDAR, DEMNAS, and TerraSAR terrain-based flood models are first tested using historical hydrological data in order to judge their sensitivity and to select which DEM produces the most reliable result. Prior to that, the DEM data are also corrected by extracting the levelling data to obtain new river depths. The flood model is simulated with a combination of 40-m grid spacing for floodplain area and finer grid spacing concerning river dimension due to computation requirements. To enhance model reliability, the model with selected DEM is then calibrated and validated by adjusting Manning's roughness coefficient (n).

Essentially, the calibrated and validated flood model will then be used as a basis for flood hazard simulations for various return period scenarios. There are three flood model scenarios for mapping flood extent: fluvial flood, tidal flood, and combined flood. Each model will display the results of the analysis of the inundation area and flood depth. In the end, by overlaying model outputs (flood intensity and land subsidence rate), the final result of this research is the mapping of flood hazards induced by land subsidence.

3.1 Data preparation

3.1.1 Hydrological data

HEC-RAS 2D hydraulic mode is utilized for hydraulic modelling. The flexibility to convert file formats in both directions between GIS and the model, as well as its availability for free, are factors in the decision to use this 2D model. Data processing with the HEC-RAS model begins with geometric data input using the HEC-RAS extension based on DEM and geometric data. Geometric data are represented by cross sections, flow paths, bank lines, and Manning's roughness coefficient. Furthermore, cross sections are very important input data because they improve terrain characterization.

In the case of hydraulic modelling, the model area is represented by 6 hydrograph designs flowing in flood-prone areas of Semarang City. The selection of the hydrographs refers to national priority rivers that must be managed in Indonesia (BPDAS, 2015) consisting of Bringin, Silandak, Siangker, Banjir Kanal Timur, Tenggang, and Babon River. In the steady flow analysis, defining the values of upper and lower boundary conditions for the stations in the model area is a crucial step. As upper boundary conditions, the maximum flood discharge can be categorized into three types: high (5-year-return period), medium (25-year-return period), and low occurrence (50-year-return period). Hydrograph design in 50-year return period is employed (Fig. 4).

The purpose of the post-processing is to process the water levels for specific cross-sections and produce a surface model of the water levels in TIN format. The water depth is created by intersecting the TIN terrain model and the TIN water level model. Flow velocity rasters are also produced from the field of cross-cutting velocities in specific cross-section profiles or their components, in addition to water depth rasters.

3.1.2 Landcover and DEM

Landcover for the study area is acquired from the GEE Landcover Classification System (LCCS) database with a supervised approach method which is based on the Sentinel2-m. Moreover, the 10 m Sentinel-2 latest satellite data is used for flood hazard mapping and to identify potential land cover damage. The data utilize Sentinel-2 images in 2022. To choose the clearest image, a cloud filter has to be applied to the image before processing

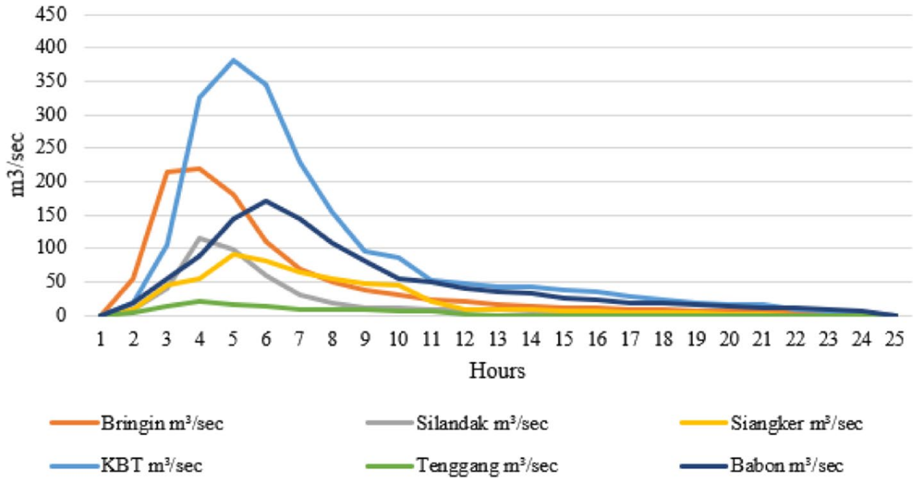

Fig. 4 Hydrograph design of six rivers in 50-year return period

begins. To lessen the impact of the cloud, our study employs a straightforward smilecart method from the Earth Engine package. This program chooses the lowest range of cloud scores at each location from a set of several temporal pictures. From the acceptable pixels, it produces per-band percentile values. A total of 30 samples from each class are chosen randomly and under supervision. Landcover consists of four classes including waterbody, settlement, vegetation, and vacant lot. The GEE's classifier function is used to carry out the classification process. Data validation using a confusion matrix has been used in other studies. A confusion matrix is a built-in algorithm in GEE that validates and evaluates the classification accuracy of the images.

Various DEMs with different spatial resolutions are utilized in this study, including LIDAR DEM, DEMNAS, and TerraSAR. These DEMs have resolutions of 1-m, 8-m, and 9-m, respectively which covered Semarang City. According to Wedajo (2017), the LiDAR DEM is particularly well-suited for precise and detailed flood modelling, especially in urban regions and areas with flat terrain. DEMNAS stands for the national DEM for Indonesia, which is a combination of multi-DEM from TerraSAR, IFSAR, ALOS PALSAR, and mass points (Atriyon and Djurdjani 2018). Besides, TerraSAR should be suitable for urban flood detection because of its high resolution in strip map/spotlight modes (Mason et al. 2010). The DEM sensitivity analysis is conducted by comparing flood extent in each DEM with the flood events in Semarang City. All DEMs have data acquisitions in the year 2014 with vertical coordinate reference system using Earth Gravitational Model 2008 (EGM2008). Considering the highly dynamic changes in terrain due to the influence of land subsidence, it is necessary to correct the DEM using the latest land subsidence rates.

3.2 Land subsidence

Land subsidence is a condition where vertical displacement occurs against a certain height reference (Abidin et al. 2010). Land subsidence data are derived from Sentinel 1 data from 2017–2020 with DinSAR method. DinSAR is a method of obtaining two paired SAR images that involves combining complex image information from either the same location or a slightly different location within the same area. This process involves the multiplication of multiple sets of conjugate images, which leads to the creation of a digital elevation model (DEM) or the detection of displacement in the Earth's surface (Prasetyo et al. 2013). The basic concept of the DinSAR method is to utilize coherence in phase measurements in obtaining distance differences and changes in distance from two or more SAR images that have complex values from the same area (Prasetyo et al. 2018). Rate of land subsidence is calculated using average differences of vertical heights of two consecutive years during the period 2017–2020. See Eq. (1).

$$\left(\frac{D_{2018-2017}+\Delta_{2019-2018}+\Delta_{2020-2019}}{3}\right)=\vartheta/\mathrm{yr} \tag{1}$$

where Δ is vertical displacement in each year, and ϑ is land subsidence rate per year. Rate of land subsidence is important to update DEM. To generate DEM correction Eq. 2 is used (Ward et al. 2011).

$$\mathrm{DEM}_{t(x)}=\mathrm{DEM}_{t(0)}-\left(\vartheta*\left(t_x-t_0\right)\right) \tag{2}$$

where $\mathrm{DEM}_{t(\mathrm{x})}$ is the DEM at a certain time (t) (i.e., year x), $\mathrm{DEM}_{t(0)}$ is the DEM in the baseline year (t_0) and ϑ is the spatially differentiated annual rate of subsidence in cm year^{-1}. The use of this method allows for a simple reassessment of the future DEM as updated and improved estimates of spatial and temporal subsidence rates.

3.3 DEM sensitivity analysis selection

It is critical to evaluate the contribution of various conditioning elements to flood modelling in order to assess a model's dependability. The choice of DEM is one of the most important aspects of flood modeling. In that respect, before carrying out proper flood model calibration and validation, the flood model's sensitivity to various digital elevation models (DEMs), including the 9-m TerraSAR, 8-m DEMNAS, and 1-m LiDAR, is evaluated using the assumption of equal river Manning's roughness coefficient of 0.06 and floodplain's roughness coefficient, as shown in Table 1. Furthermore, simulations are carried out using Q50 and HHWL as upstream and downstream boundary conditions respectively, based on

Table 1 Manning's n (roughness coefficient) for different land covers and channel characteristics

Land cover	Manning's n
Forest	0.1
Built-up area	0.013
Open spaces	0.027
Maritime wetlands	0.04
Mine	0.013
Arable land	0.03
Channel	Manning's n
Uniform firm soil bed: Bringin, Silandak, Siangker, Tenggang, and Babon	0.025*
Uniform firm soil bed with obstruction: Banjir Kanal Timur	0.025–1.6**

*Manning's n value is uncalibrated due to flood event image data unavailability and scarcity

**Scenarios for validation of additional adjustment factors for channel's n values based on Arcement (1989) which was the modified version of (Aldridge, 1973)

Indonesia's Minister of Public Works and Housing statement referring to the 50-year return period storm event in February 2021 (https://www.bbc.com/indonesia/indonesia-56007558, accessed August 2023). This model is then compared to flood2020 and flood2021 events from Semarang City's Regional Agency for Disaster Countermeasure (BPBD) data and field survey. The terrain that produces the best fitting result will then be used in subsequent flood modeling calibration and validation procedures.

We choose four confusion matrix measures to assess the four models' performance: accuracy (A), precision (P), recall (R), and F-score (F). These confusion matrices have been commonly adopted by a substantial portion of researchers, including references (Li et al., 2019; Razali et al. 2020), for the prediction of flood risks. In summary, accuracy measures overall correctness, precision focuses on correct positive predictions, recall assesses the model's ability to find all positive instances, and the F-score reveals balances precision and recall. These indicators may serve as a gauge of how well the model captures the dangers associated with flooding.

$$P=\frac{\mathrm{TP}}{\mathrm{TP}+\mathrm{FP}} \tag{3}$$

$$R=\frac{\mathrm{TP}}{\mathrm{TP}+\mathrm{FN}} \tag{4}$$

$$A=\frac{\mathrm{TP}+\mathrm{TN}}{\mathrm{FP}+\mathrm{TP}+\mathrm{TN}+\mathrm{FN}} \tag{5}$$

$$F=\frac{2\times P\times R}{P+R} \tag{6}$$

where TP (true positive) is the proportion of samples that is accurately classified as flooding floodplain; TN (true negative) is the proportion of samples that is accurately classified as non-flooding floodplain; FP (false positive) is the proportion of samples that is incorrectly classified as flooding floodplain; and FN (false negative) is the proportion of samples that is incorrectly classified as non-flooding floodplain.

3.4 Flood modelling

A two-dimensional HEC-RAS model is used in modelling the flood inundation extent. The model takes into account hydrodynamics, horizontal and vertical flows, and 2D flow visualization—things that a 1D model cannot solve (Dasallas et al. 2019). A finite-volume algorithm allows for the use of a computational mesh. With this approach, the wetting and drying of 2D elements are particularly resilient. A rapid surge of water can be handled in 2D Flow Areas visualized by grid cells, which can start off dry. The algorithm can also handle mixed flow regimes (flow crossing past critical depth, like a hydraulic leap), supercritical, and subcritical flow regimes (Brunner et al. 2015).

The stage-storage relationships of floodplains in the simulation grid cells are obtained from the terrain or DEM information, allowing for bigger computational cells without sacrificing landscape details. As for the channel, the terrain is built based on cross-sections at multiple locations along the channel. Both the floodplain and the channel are linked using a lateral structure, in this case, levees to better depict the existing condition. All of those components are then calculated using 2D flow areas that serve as the basis for the hydraulic geometry.

While HEC-RAS is capable to accommodate both diffusion wave and Saint Venant equation set, for tidal-influenced flood conditions, it is recommended to use a 2D Saint Venant equation rather than a 2D diffusion wave equation set to better capture the propagation of waves into a river system (Brunner 2016). Hence relevantly, the usage of Saint Venant equation is usually recommended in a case such as this study which utilizes a tide stage hydrograph as a downstream boundary condition. However, it is also important to note that the 2D diffusion wave equation's running time is much faster and generally has better stability than the 2D Saint Venant (Martins et al. 2017; Quiroga et al. 2016). Given that both techniques are initially tested, they produce results that are remarkably similar, particularly in the study area, the floodplain area. This is due to the insignificant gap between the high highest water level (HHWL) tide and river flood water, so the wave propagation effect as well as the backwater effect are almost inevident, producing nearly identical results. Thus, a 2D diffusion wave is chosen over a 2D Saint Venant equation set. The 2D diffusion wave equations are as follows (Brunner et al. 2015):

$$\frac{\partial H}{\partial t} + \frac{\partial (hu)}{\partial x} + \frac{\partial (hv)}{\partial y} + q = 0 \tag{7}$$

$$g\frac{\partial H}{\partial x} + c_{\mathrm{f}}u = 0 \tag{8}$$

$$g\frac{\partial H}{\partial y} + c_{\mathrm{f}}v = 0 \tag{9}$$

$$c_f = \frac{g|V|}{M^2R^{4/3}} \tag{10}$$

where H is the surface elevation (m); h is the water depth (m); u and v are the velocity components in the x- and y-directions respectively (ms^{-1}); q is a source/sink term; g is the gravitational acceleration (ms^{-2}); c_{f} is the bottom friction coefficient (s^{-1}); R is the hydraulic radius (m); $|V|$ is the magnitude of the velocity vector (ms^{-1}); and M is the inverse of Manning's n (m(1/3) s^{-1}).

Following advice from the HEC-RAS River Analysis System 2D Modelling User's Manual, Manning's n is assigned following the type of land cover. Therefore, Manning's n value for each land cover is assigned based on Chow (1959) whereas for the channel and floodplains Manning's n value is derived from the United States Geological Survey's guide written by Arcement (1989) due to its further consideration on adjustment factors (Table 1).

3.5 Evaluation of flood modelling performance

The comparison of observed flood images using satellite and flood simulation is commonly used to evaluate the performance of the flood model with channel and floodplain's Manning's roughness coefficient (n) as the calibrated variable (Horrit et al. 2007, Di Baldassarre et al. 2009, Liu et al. 2019). In this study, the progression of the channel's n value for the model's calibration is based on adjustment factors stated in Arcement (1989), which

Table 2 Flood scenarios based on boundary conditions

Boundary condition	Fluvial flood	Tidal flood	Combined
Upstream: river Discharge	Q_5, Q_{25}, Q_{50}	Q_{initial}	Q_5, Q_{25}, Q_{50}
Downstream: tidal	Mean sea level	High highest water level	High highest water level

take into account the channel's degree of irregularity, obstruction, and vegetation. Importantly, this method is limitedly used only to evaluate the fluvial flood at Banjir Kanal Timur (Table 1), especially based on the January 1st—January 2nd, 2022 flood event (referring to the news: https://radarkudus.jawapos.com/jateng/02/01/2022/pergantian-tahun-warga-semarang-ditemani-banjir/).

The Sentinel-2 satellite imagery process is utilized under GEE using the NDWI method to derive the observed flood extent on the respective date and location. Using the same date's river discharge record as an upstream boundary condition, which is obtained from BBWS Pemali Juana, this flood extent is then compared with the modelled flood. Concerning the validation of model results in other rivers, such data are regrettably either scarce or unavailable for the model area, a problem commonly found in similar studies (Apel et al. 2009, Vojtek and Vojteková 2016). Therefore, as for the tidal flood, 20th–29th of February 2020 Sentinel 2 satellite imagery is used to evaluate the performance of the flood model (referring to the highest IOC tidal data in 2020), especially near the coastal area. The tidal boundary conditions used for flood modelling refer to 2020 observation (Andnur 2022) (more explanation see **3.6**).

The flood model's performance is evaluated using a measure of fit F index (Horrit et al. 2007, Quiroga et al. 2016, Liu et al. 2019) and C Index (Liu et al. 2019) with equations as follows:

$$F = \left(\frac{A_{\text{om}}}{A_{\text{o}} + A_{\text{m}} - A_{\text{om}}} \right) \tag{11}$$

$$C = \frac{A_{\text{om}}}{A_{\text{o}}} \tag{12}$$

A_{o} refers to the observed flooded area, A_{m} is the modelled flooded area, and A_{om} refers to the fit between both the observed and the modelled flooded area. Both F and C range from 0 to 1 with a value closer to 1 meaning better performance. However, it is important to note that higher F needs to be prioritized rather than higher C concerning how F indicates a degree of how perfectly the model matches the observed event, while C just represents the percentage of correctly predicted flood map extent area.

3.6 Flood scenarios

In this study, three flood scenarios are simulated to better understand the pattern and occurrence of hazards derived from their sources, upstream (river discharge hydrograph) and/or downstream (in this case: tidal elevation) which are set through the HEC-RAS boundary condition. These scenarios are explained and shown in Table 2.

Q_5, Q_{25}, and Q_{50} refer to 5-year, 25-year, and 50-year return period discharge hydrographs respectively (Semarang drainage master plan, 2020) while Q_{initial} is an average discharge value in the wet season derived from the automated water level recorder (AWLR) river discharge measurement closest to the study area obtained from BBWS Pemali Juana. Furthermore, the mean sea level (MSL) and high highest water level (HHWL), 185.2 and 277.7, respectively, are modified from Andnur (2022). The boundary condition for HHWL is +0.925 referring to the difference between Andnur (2022)'s HHWL and MSL value.

3.7 Flood hazard categories

Flood hazard categorization in this study takes into account the factors of flood intensity (FI), classification of flood hazard, and a class of function area. Flood intensity is based on the raster of water depth (d) and flow velocity (v) for each flood scenario ($Q5$, $Q25$, $Q50$) using Eq. (13) (Drbal et al. 2009):

$$\text{FI} = \left\{ \begin{matrix} 0 \rightarrow d = 0m \\ d \rightarrow d > 0m, v \leq 1m/s \\ d.v \rightarrow v > 1m/s \end{matrix} \right\} \tag{13}$$

Considering the National Agency for Disaster Countermeasure (BNPN) Indonesia Guidelines, the flood hazard is based on the distance from the river and slope. There is no classification of flood hazard maps due to land subsidence. Therefore, in this study, we will use a classification based on Flood Intensity and subsidence rate as an indicator to determine the risk of flooding. Since the flooding strength in the flooded area is greater, the flood hazard will also be greater. Flood hazard categories are shown in Table 3.

4 Result and discussion

4.1 Land subsidence

To find out the current condition of land subsidence that occurs in Semarang, DinSAR is processed using sentinel 1A period 2017–2020. The outcome is illustrated in Fig. 5. It can be perceived that the land subsidence value is spatially and temporally distributed. Several colorless areas are found and defined as low coherence. It usually is found in areas with dense vegetation, water surfaces, or relatively flat areas. Areas that have a high land subsidence rate between 8 and 14 cm/year are generally located in the eastern region of Semarang City. For validation purposes, the results of the DinSAR processing are compared with the GPS observation methods from GPS measurements in 2017 (Wirawan et al. 2019) and (Istiqomah et al. 2020). Table 4 presents the results of the calculation of mean square error (RMSE). RMSE represents DinSAR processing overall fit to the GPS measurement, in addition to how closely the DinSAR data points match the values of the GPS measurements. From the table, it is evident that land subsidence from 2017 to 2018 has an RMSE value of 2.72 cm, and from 2018 to 2019 it has an RMSE value of 1.95 cm. DinSAR observations have a deviation of up to 2.7 cm compared to GNSS survey. One of the causes of the deviation is that backscatter may not be well received or interpreted accurately. This outcome can be attributed to several factors, including sensor frequency, incident angle, and terrain features such as slope, hardness,

Table 3 Classification of flood hazard induced by land subsidence categories modified from Vojtek and Vojteková (2016)

Flood intensity (FI)	Rate of land subsidence (RLS) (cm/yr)	Hazard categories	Description
$FI > 1$	$RLS \geq 9$	High	It is advised against approving new construction or additions to buildings where humans or animals reside
$0,3 < FI \leq 1$	$4 < RLS < 9$	Medium	Construction is feasible, but there are limitations based on a careful analysis of how essential certain item functions are in the vulnerable region
$FI \leq 0.3$	$RLS \leq 4$	Low	Construction is feasible, but should be aware of the potential flood risk

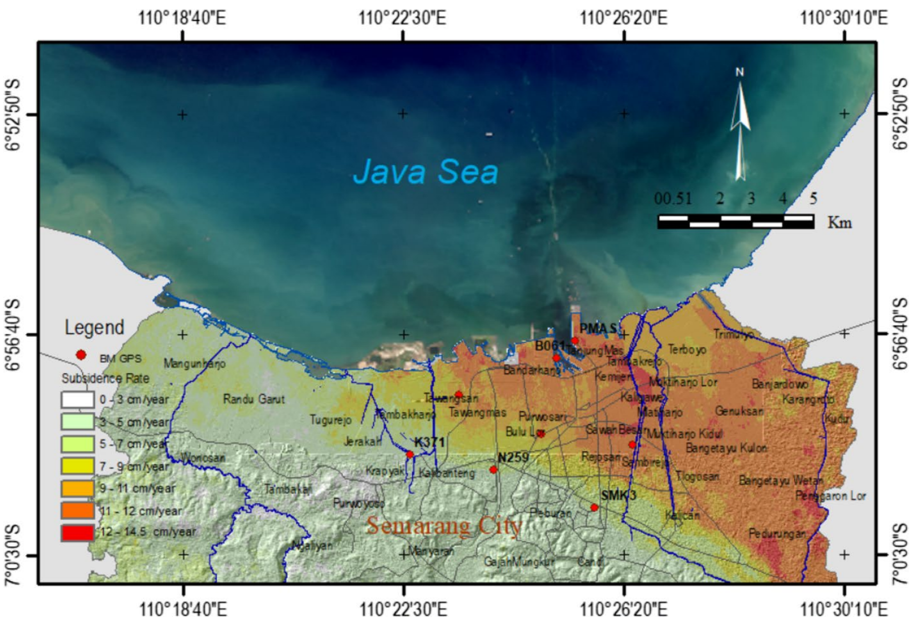

Fig. 5 Land subsidence rate 2017–2020 derived from DinSAR

Table 4 Land subsidence comparison of DinSAR and GPS method

Station	2017–2018 (cm)		2018–2019 (cm)	
	GPS	DinSAR	GPS	DinSAR
smk3	− 2,9	− 4,8	− 5,3	− 4,6
n259	− 4,6	− 2,9	− 3,6	− 4,6
k371	− 0,4	− 4,3	− 4,1	− 2,4
kop8	− 6,1	− 9,4	− 5,3	− 7,8
prpa	–	–	− 4,6	− 8,2
pmas	–	–	− 7,3	− 6,5
bugn	–	–	− 6,6	− 8,9
b061	–	–	− 7,8	− 8,6
RMSE		2,7		1,95

inhomogeneity in texture, and dielectric constant (Srivastava 2022). RMSE represents the difference between the results of DInSAR and GPS, which is generally within a few centimeters (Luo et al. 2014; Liu et al. 2015; Yastika et al. 2019). Therefore, it can be stated the DinSAR results in this study are acceptable. The rate of land subsidence has been similar to previous studies. In certain locations, land subsidence rate reaches 14 cm year^{-1}. According to Abidin et al. (2010), monitoring land subsidence has been carried out through geodetic techniques such as levelling, InSAR, and microgravity data. The research revealed that subsidence reached a maximum rate of approximately 15 cm year^{-1} between 1979 and 2006. Yastika et al. (2019) noted that specific regions experienced even more severe subsidence, measuring 24–36 cm within a two-year period from 2015 to 2017.

4.2 DEM sensitivity analysis and selection

The Regional Agency for Disaster Countermeasure (BPBD) of Semarang City's data and field survey are used to compare flood2020 and flood2021 occurrences to the 50-year return period flood model employing all TerraSAR, DEMNAS, and LiDAR. Simulations of flood inundation using TerraSAR (Fig. 6a) and DEMNAS (Fig. 6b) show that flood is not found in the middle part of northern Semarang. However, it is quite clear that the spatial distribution of flood depths reaching a fairly high depth ranging from 1.0—1.5 m is found in the northern area of the Mangkang, Randusari Tugurejo, and Tambakharjo. To the north of Genuk district, such as in Terboyo and Trimulyo, characteristics of the flood depth in the inundation are almost similar based on both DEM models. However, for simulation using LiDAR DEM (Fig. 6c), significant flood extent with depths ranging up to 1.5 m is spatially distributed at Mangkang, Rangdugarut, Tugurejo, Tanjung Mas, and Terboyo dan Trimulyo with elevation of terrain lower than MSL (mean sea level).

Table 5 shows that the simulated flood extent areas for the DEMNAS and TerraSAR DEMs are not much different, while the model using LiDAR-based terrain produces almost double the extent. It is important to note that all the models produce maximum velocity ranging closely between 1.4 and 1.6 m s^{-1} which proves how all the terrain scenarios have an almost similar flat sloping despite the different elevations. Velocity sensitivity analysis shows that simulated flood velocity is lower for the DEMNAS, while LiDAR and TerraSAR velocities do not show significant differences. The modelled velocity depends on the maximum depth, where a higher depth corresponds to a higher velocity. However, the velocity does not affect the extent of the inundation. The extent of inundation is greatly influenced by the accuracy of the digital elevation model (DEM) used. A more precise DEM will provide higher accuracy in determining the extent of inundation. Moreover, the extent of inundation as well as its accuracy is highly related to flow accumulation which is further explained in Appendix 1.

In this study, the assessment of DEM performance relies on confusion metrics such as model accuracy, precision, recall, and the *F*-score. These confusion matrices have been commonly adopted by a substantial portion of researchers, including references (Li et al. 2019; Razali et al. 2020), for the prediction of flood risks. Overall, the results show that the accuracy of LiDAR DEM (88%) is better than other DEMs which are DEMNAS (23%), and TerraSAR (31%). DEM sensitivity analysis depicts that the DEMNAS 8.1-m and TerraSAR 9-m have terrain errors and cannot be used in representing the floodplain in Semarang City. However, the analysis of flood extent using LiDAR 1-m shows a rather satisfying ratio of correctly predicted area. Therefore, LiDAR 1-m is selected to be used for flood modelling in this research.

4.3 Evaluation of flood model performances

One of the most important factors that imply flood dynamics is the selection of channel's *n* values which are derived not only from bed material but also the channel's cross-section geometry, as well as obstruction and vegetation characteristics. For each selected channel Manning's *n* ranges from 0.020 to 0.08 is simulated to illustrate the correlation between the channel's roughness coefficient and model performances measured by *F* and *C*. As can be seen in Fig. 7, both models' fitness generally increases as channel's *n* progresses. Additionally, the model reaches its peak stagnant performances in Manning's *n* range of 0.05–0.06, 0.3 higher than its initial Manning's value which is portrayed as a fully clean unobstructed

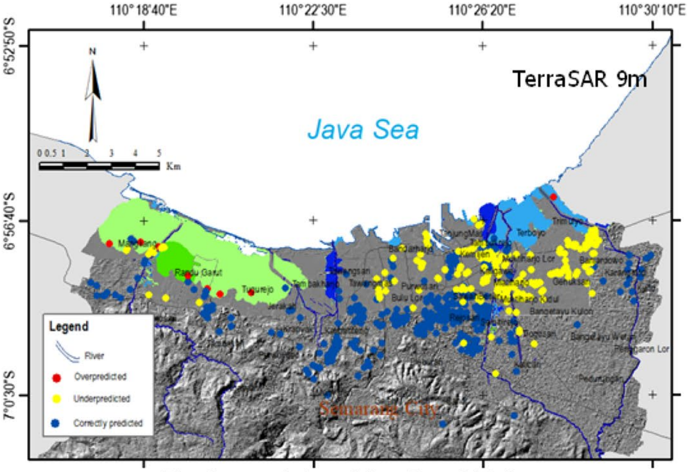

a. Flood extent derivated from TerraSAR 9-m

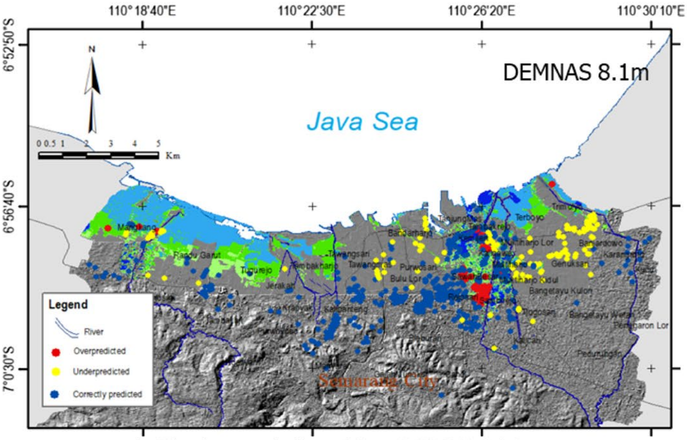

b. Flood extent derivated from DEMNAS 8.1-m

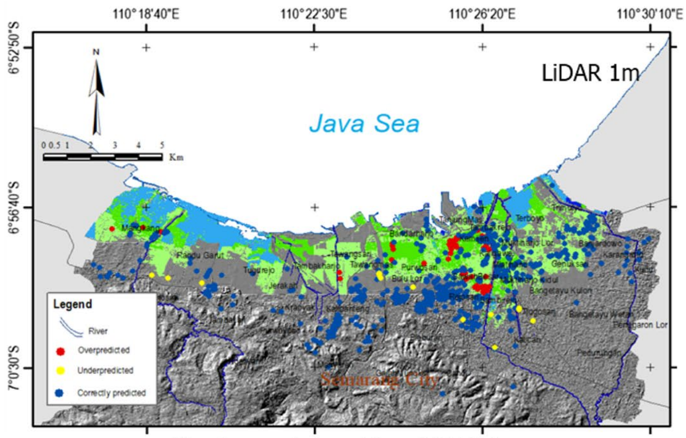

c Flood extent derivated from LiDAR 1-m

Fig. 6 Flood model sensitivity analysis against various DEM **a** 9-m TerraSAR **b** 8.1-m DEMNAS and c. 1-m LiDAR

Table 5 Flood model sensitivity

No	DEM	Maximum depth (m)	Velocity (msec^{-1})	Flood extent (Km2)	Precision	Recall	Accuracy	*F* Measure
1	TerraSAR-X	2.38	1.56	22.4	0.11	0.64	0.31	0.19
2	DEMNAS	1.50	1.43	27.38	0.57	0.41	0.23	0.47
3	LiDAR	1.95	1.54	42.03	0.74	0.94	0.88	0.83

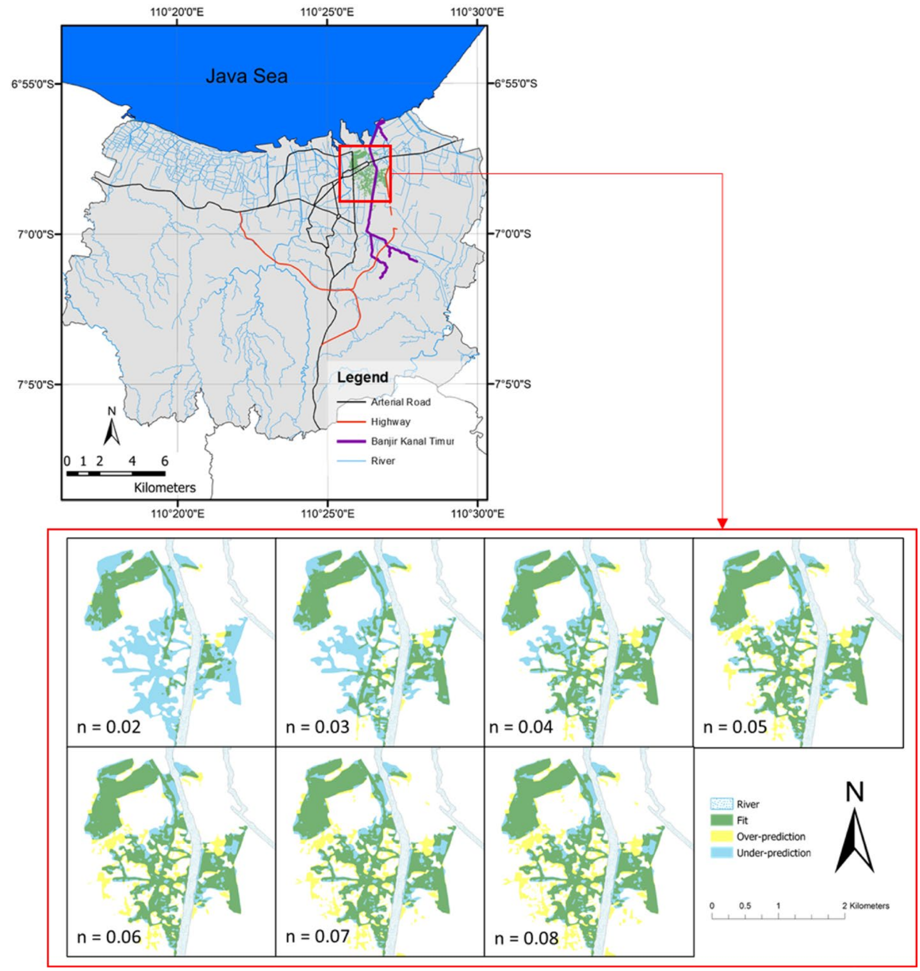

Fig. 7 Model fitness of Banjir Kanal Timur's flood model with different manning's *n* values

firm soil bed stream. This is probably caused by the fact that Banjir Kanal Timur's cross-sectional area (by validation period), despite its homogeneous topography and typical normalized cross-section, is occupied by a decent part of sediment which impacts the variation of the channel cross-section and intensifies the effect of obstruction. Table 5 summarizes

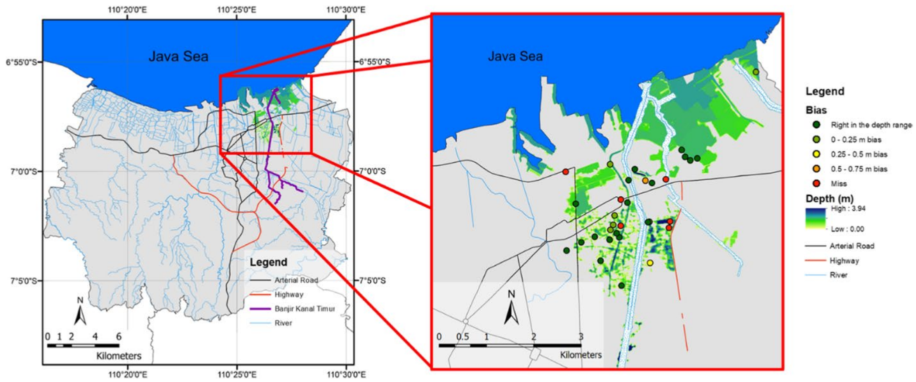

Fig. 8 Model fitness of Banjir Kanal Timur's flood based on the depth range

the *F* and *C* scores for each Manning's *n*. As for the *F* indexes, model evaluations provide measures of fit values higher than 0.6 for Manning's *n* same or higher than 0.05. Hence, Manning's *n* of 0.06 which produces the best *F* performances is selected as the final roughness coefficient for Banjir Kanal Timur.

The model fitness of Banjir Kanal Timur's flood model is further evaluated based on depth range data which are collected using primary survey in the same area and time period (Fig. 8). It can be seen that although there are a handful of over-predicted or under-predicted spots (represented by red dots), the fitted spots generally show accurate flood depth. It implies that the DEM generated using the LiDAR can give accurate representation of the actual terrain in a particular time period while on the other hand still vulnerable to the micro-scale accuracy of water infrastructure such as levee and drainage channels which are not or hardly represented in the model.

On the other hand, the performance of the tidal flood model is evaluated more straightforwardly by comparing the modelled flood utilizing land cover Manning's *n* as stated in Table 1 to the historical flood as explained in Sect. 3.4. For the most part, the model (Fig. 9) tends to overestimate the flood event, especially in Mangunharjo, Karanganyar, and Tugurejo areas. Despite that, it still produces relatively good *F* scores of 0.79 and *C* scores of 0.95 (Table 6).

Evaluations of both flood models generally produce satisfactory results with an F score higher than 0.6, the minimum value accepted by other studies (Quiroga et al. 2016, Horrit and Bates 2002, Horrit et al. 2007, Baldasarre et al. 2009). Despite that, the limitation of the model is generally divided into two categories: the uncertainties produced by using unsupervised satellite imagery as the benchmark observed flood extent and detailed terrain and geometry factors that cannot be thoroughly depicted by the model. As for Banjir Kanal Timur's case, a remotely sensed flood event cannot differentiate whether the flood surrounding the stream is caused by the overflowing of the river or is influenced by local drainage problems which are also commonly found in the area. Not to mention because of the endogenic processes on the observed flood cells, any additional precipitation will get ponded once the ground is saturated. Furthermore, the limitation of this performance evaluation is also due to the unavailability of several parts of river cross-sections in Semarang City including levees' technical geometry details. Although river geometry interpolation has already been carried out, the full availability of river cross-section will surely increase the representation of the riverbed in the DEM which in turn can increase the output of the

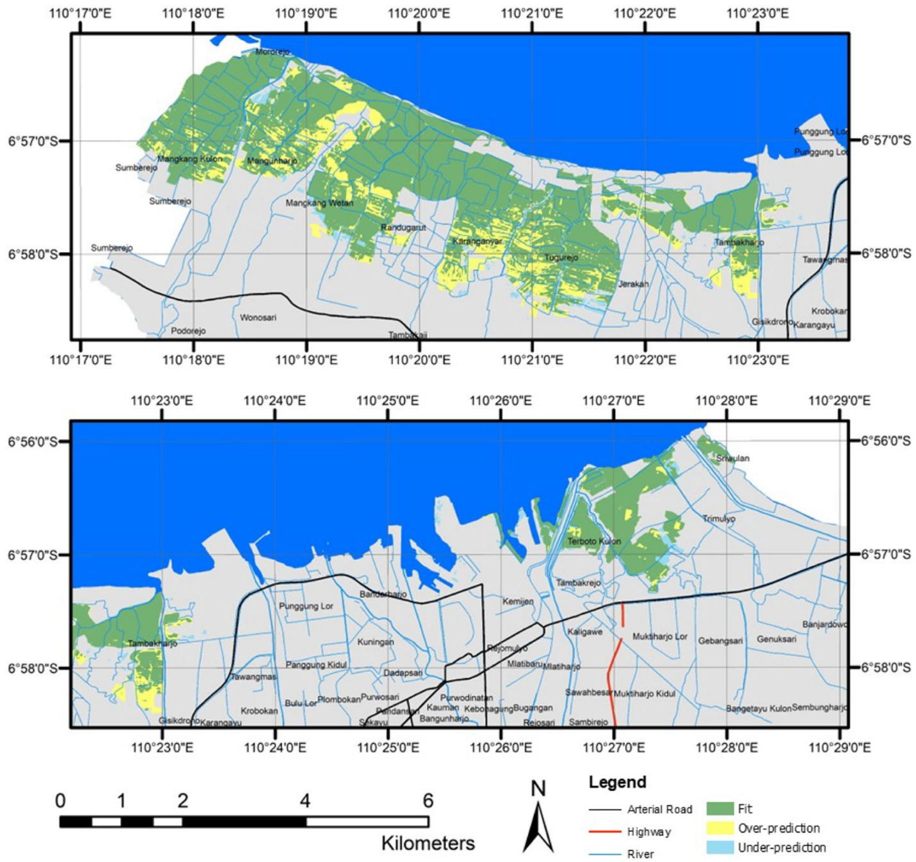

Fig. 9 Model fitness of tidal flood model in each administrative area

Table 6 Performance of the Banjir Kanal Timur flood model with different channels' manning's n

Manning's n	A_o (km^2)	A_m (km^2)	A_{om} (km^2)	F-Index	C-Index
0.02	2.193	0.745	0.687	0.31	0.31
0.03	2.193	1.282	1.148	0.49	0.52
0.04	2.193	1.685	1.461	0.60	0.67
0.05	2.193	2.048	1.642	0.63	0.75
0.06	2.193	2.233	1.713	0.63	0.78
0.07	2.193	2.378	1.751	0.62	0.80
0.08	2.193	2.468	1.770	0.61	0.81

model including flood extent and depth of inundation. On the other hand, the similar pattern of tidal flood model overestimation in most administrative areas is most likely caused by mutable ponds and man-made emergency levees spreading across maritime wetlands that are hardly included in the model.

4.4 Model sensitivity

Outputs of hydrological modelling include flood inundation, velocity, and flood extent. The model is simulated for designed flood events of 5-, 25-, and 50-year return periods with flood scenarios namely tidal, fluvial, and combined floods. Figure 10 shows flood extent and inundation depth in the fluvial scenarios for 5-, 25-, and 50-year designed events and tidal scenarios. Using 5-year return period most of affected areas experience combined flood with depths less than 0.5 m and between 1.0 and 1.5 m. Figure 10a) shows that flood happens in Tugu district with most areas having flood depth ranging from 1.0 to 1.5 m. In Semarang Utara district, the majority of flood happens in center part of the area with <0.5 m flood depth. In West Semarang and Gayamsari districts, the depth ranges around 0.5 m. In Genuk district, several areas have an inundation depth around 1.5 m such as Trimulyo, Terboyo Kulon, and Terboyo Wetan villages. The 25-year return period (Fig. 10b) and 50-year return period (Fig. 10c) show similarities. There are six areas that are inundated by combined flood: Tugu, West Semarang, North Semarang, East Semarang, Gayamsari, and Genuk districts. Most areas have depth ranging from 1.0 to 1.5 m in Tugu, and <0.5 m flood depth is found in Semarang Barat, Semarang Utara, Semarang Timur, Gayamsari, and Genuk districts, and only few areas have depth ranging 1.0–1.5 m (Terboyo Kulon, Terboyo Wetan and Trimulyo).

Details of flood inundation depth areas against designed flood events of 5-, 25-, and 50-year return periods are given in Table 7. In terms of the fluvial flood, the flood extent increases as the flow hydrograph scenario progresses from $Q5$ to $Q50$. The $Q5$ scenario has the highest ratio of flood extent with a depth of less than 0.5 m, reaching 77%, while the $Q25$ and $Q50$ scenarios have a ratio that is 12% lower. However, in the flood depth range of 0.5–1.0 m, the situation is reversed, with $Q25$ and $Q50$ ratios equalling slightly more than 30% and Q5 ratios reaching around 20%. Furthermore, in contrast to the tidal and combined flood simulation results, only a minor extent of flood with a depth of more than 1 m is found under the fluvial flood event category by a maximum of only up to 1.69 km2 (5% ratio) under the $Q50$ scenario. This could indicate the significant contribution of tidal flooding as well as land subsidence on the overall flood conditions in Semarang. The tidal flood areas do not change in 5-, 25-, and 50-year return period scenarios because tidal flood only considers the high highest water level (HHWL) factor, without considering flood discharge in each return period. The inundation area with a depth of more than 0.5 m caused by tidal flood is wider compared to its counterpart caused by fluvial flood in 5-, 25-, and 50-year return periods.

As for the combined flood, the total flood extent in each return period is increasing. The extent reaches 39.09, 41.02, and 42.03 in 5-, 25-, and 50-year ARI (Annual Recurrent Intervals), respectively. It increases linearly with increase in each inundation depth. Figure 11 shows that the average increases in inundation area according to the depth of 0.0–0.5 m, 0.5–1.0 m, 1.0–1.5 m, and 1.5–2 m are 1.9%, 1.2%, 0.4%, and 0.2%, respectively. The widest inundation area is at a depth of 0.0–0.5 m reaching 21.53 km^2 under the 25-year-return-period.

Table 8 shows that the flood velocity in 5- and 25-year return periods is less than 1.5 m/s. However, it reaches up to 1.53 m/s in 50-year return period. The velocity and extent of flooding at the 50-year return period have the highest values compared to other return periods.

Flood intensity refers to the severity or strength of a flood event. It is a measure of the magnitude of flooding in terms of the volume of water, the rate of water flow, the depth

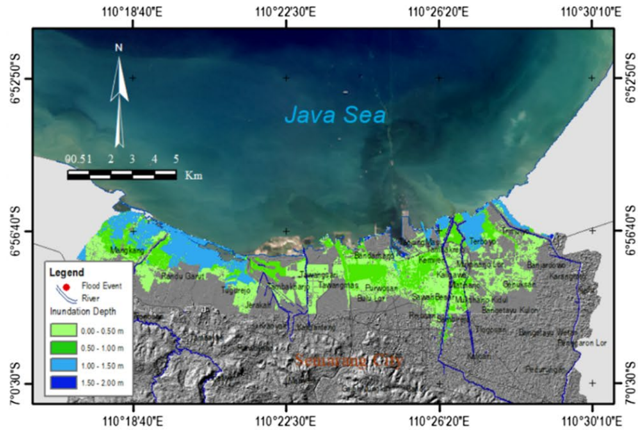

a. Combined flood 5-year return period scenario

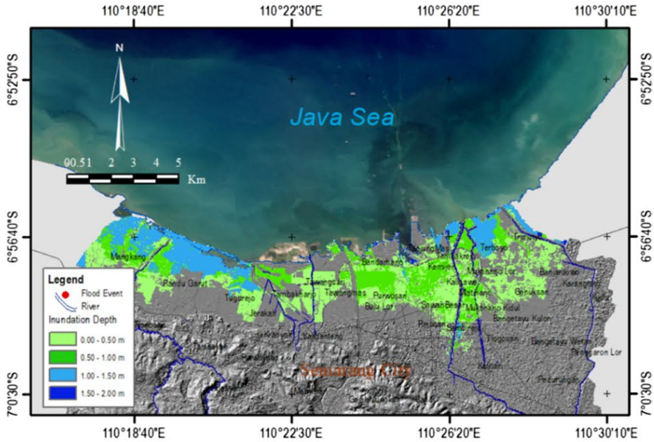

b. Combined flood 25-year return period scenario

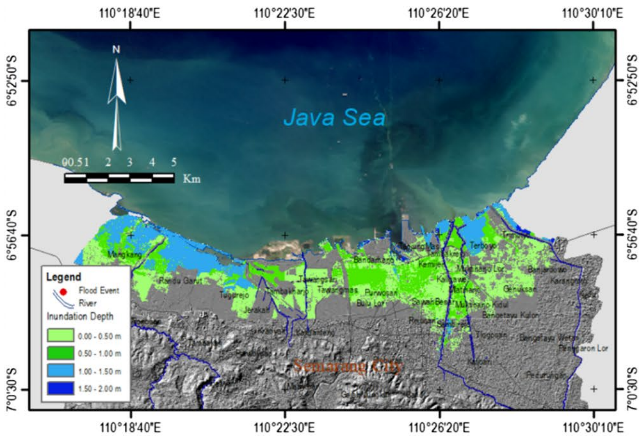

c. Combined Flood 50-year return period scenario

Fig. 10 Simulated depth and inundation extent in combined flood periods **a** 5-year, **b** 25-year, **c** 50-year return period scenario

Table 7 Flood model sensitivity in various annual recurrent intervals based on inundation depth

Inundation depth	Fluvial flood		Tidal flood		Combined	
	Area (km^2)	(%)	Area (km^2)	(%)	Area (km^2)	(%)
Q5						
0.00–0.50 m	22.58	76.64	12.57	46.82	20.18	50.88
0.50–1.00 m	6.46	21.93	5.54	20.61	10.16	25.62
1.00–1.50 m	0.41	1.39	8.70	32.4	9.16	23.11
1.50–2.00 m	0.01	0.04	0.05	0.17	0.15	0.39
Total	29.46	100	26.86	100	39.65	100
Q25						
0.00–0.50 m	21.60	65.8	12.57	46.82	20.99	50.99
0.50–1.00 m	10.61	32.32	5.54	20.61	10.51	25.54
1.00–1.50 m	0.59	1.79	8.70	32.4	9.44	22.95
1.50–2.00 m	0.03	0.09	0.05	0.17	0.21	0.52
Total	32.83	100	26.86	100	41.15	100
Q50						
0.00–0.50 m	22.24	64.45	12.57	46.82	21.55	51.11
0.50–1.00 m	11.56	33.5	5.54	20.61	10.85	25.72
1.00–1.50 m	0.63	1.83	8.70	32.4	9.48	22.49
1.50–2.00 m	0.08	0.22	0.05	0.17	0.29	0.69
Total	34.51	100.00	26.86	100.00	42.17	100.00

of inundation, and the destructive potential it poses to the affected area. Flood intensity in 50-year return period scenario is shown in Fig. 12. High zone of flood intensity of tidal flood (Fig. 12a) has a higher value than its corresponding area in fluvial flood (Fig. 12b). Fluvial flood with wider inundation can be found in northern Tugu and northern Genuk districts. Most of Tugu district is dominated by areas that have elevations lower than MSL (mean sea level). However, the Genuk district has experienced a high rate of land subsidence, which exacerbates the impact of flood intensity, especially in the northern and western parts of the Genuk district. In combined flood (Fig. 12c), floodplain in urban areas

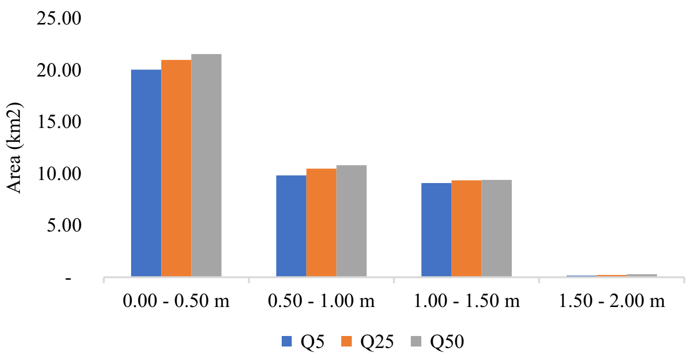

Fig. 11 Potential flood extent against inundation depth in combined flood

Table 8 Flood model sensitivity to return period, maximum depth, and velocity in combined flood scenario

No	Return periods	Maximum depth (m)	Velocity (m/s)	Flood extent (Km^2)
1	5-year	1.688	1.339	39.09
2	25-year	1.877	1.416	41.02
3	50-year	1.947	1.535	42.03

located on a river experiences a fairly high discharge, such as the Banjir Kanal Timur (BKT) and the Bringin River, indicating moderate and high flood intensity flood hazard. This condition is exacerbated because most floodplain areas are predominantly found in low elevations, especially areas adjacent to rivers.

4.5 Land subsidence and inundation depth

Low land subsidence rates are observed in terrains with low-elevation terrain below sea level, resulting in high water inundation in Mangkang. On the other hand, areas with low subsidence rates in high-elevation terrains have low water inundation heights, such as in Tambakharjo. Kemijen which has terrain elevation of approximately 0.4 m shows relatively high land subsidence rate, leading to moderate flood depths ranging from 50 to 70 cm. Areas with high flood water inundation heights (>1 m) are found in Terboyo and Trimulyo, where not only are the terrains low below sea level, but they also experience high subsidence rates. Inundation depths related to land subsidence rate and terrain elevation are shown in Table 9.

The correlation between land subsidence, DEM, and flood depth can be summarized and categorized into three types as follows:

1. Land subsidence and DEM: The terrain's elevation, represented by the DEM, plays a crucial role in land subsidence. Areas with low elevations below sea level are more susceptible to land subsidence. When the land subsides in such regions, it exacerbates the flooding problem since the relative sea level rises, increasing the chances of water inundation during floods.
2. Land subsidence and flood depth: The rate of land subsidence directly impacts the flood depth during inundation events. Higher subsidence rates in an area will lead to a more significant decrease in the land's elevation over time, resulting in a higher relative sea level during floods. Consequently, floodwaters can reach greater depths in areas experiencing substantial land subsidence.
3. DEM and flood depth: The DEM, which provides information about the terrain's elevation, is directly related to flood depth. Lower elevation areas, as represented by the DEM, are more likely to experience higher flood depths during inundation events. Higher elevation areas, on the other hand, will generally have lower flood depths during the same flooding events.

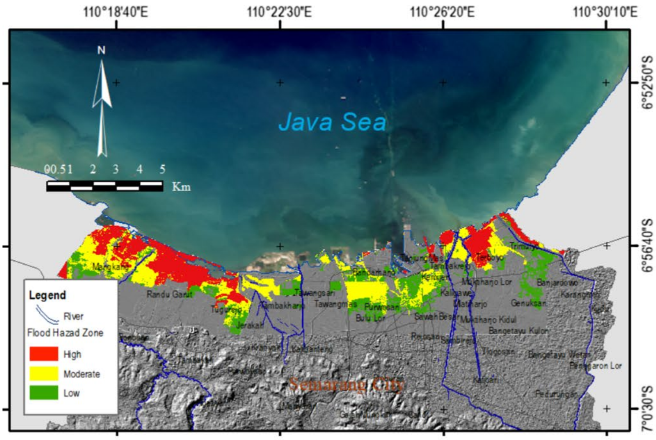

a. Tidal flood intensity

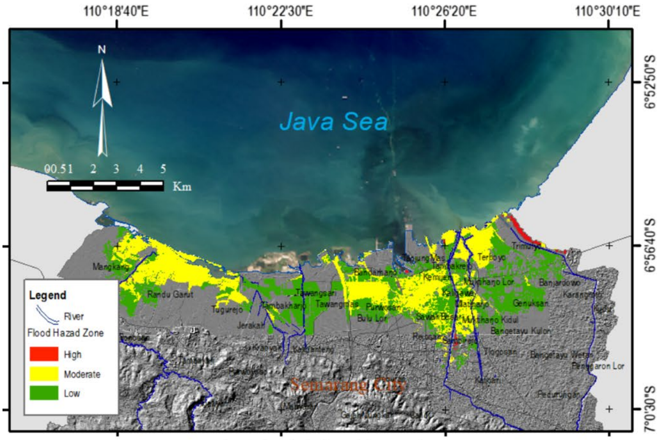

b. Fluvial flood intensity

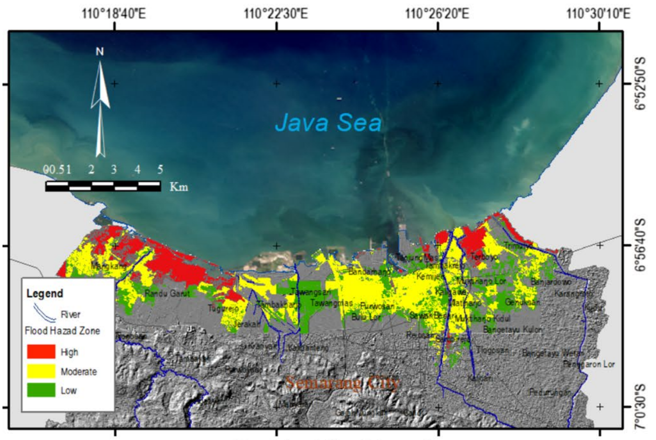

c. Combined flood intensity

Fig. 12 Flood intensity in 50-year return period **a** Tidal **b** Fluvial and **c** Combined flood

Table 9 Characteristics of inundation depth related to land subsidence and terrain elevation

No	Location	District	Terrain elevation (m)	Inundation depth (m)	Rate of land subsidence (m yr^{-1})
1	Mangkang	Mangkang	−0.22	1.50	0.03
2	Tugurejo	Mangkang	−0.37	1.30	0.06
3	Tambakharjo	Semarang Barat	1.18	0.30	0.05
3	Bandarharjo	Semarang Utara	0.36	0.70	0.10
4	Kemijen	Semarang Timur	0.45	0.74	0.10
5	Tanjung Mas	Genuk	−0.50	1.50	0.09
6	Terboyo	Genuk	−0.40	1.50	0.09
7	Trimulyo	Genuk	−0.14	1.50	0.09

4.6 Mapping flood hazard induced by land subsidence

The flood hazard map of the study area is divided into three classes as follows: areas with high, moderate, and low hazard levels as shown in Fig. 13. The boundary conditions for the categories are evaluated referring to Table 2 with GIS method.

Tidal flood extents are triggered by tidal factors and exacerbated by land subsidence (Fig. 13a). Genuk and northern part of Semarang Utara district area fall into the high-level hazard category due to the high rates of both flood intensity caused by tidal factors and land subsidence. Contrastingly, there is no potential hazard of tidal flooding in Tawangsari and Tawangmas parts of Semarang Barat district, because most of the topographic elevation of those two areas is higher than the mean sea level elevation.

On the other hand, the areas labelled on the map as high-level hazard of fluvial flood (Fig. 13b) are strongly influenced by the river discharge according to inundation depth, velocity, and land subsidence rate, as referred to Table 3. High-level hazard of fluvial flood can be found in floodplain areas of Genuk and the east part of Semarang. Comparatively to fluvial and tidal flooding, combined flood modelling in Fig. 13c shows changes in the hazard levels. For example, for fluvial flood the hazard level in Tugu and Semarang Barat district is low, but it changes into moderate level for combined flood. For tidal flood, there is a change in Tawang Mas and Tawangsari districts from no flood found in that area into an area with low and moderate hazard levels. In the Genuk district area, both the moderate and high hazard levels expand when considering the combined flood scenario. This means that when taking into account both fluvial (riverine) and tidal flooding, a larger area in Genuk district is classified as having moderate to high flood hazards. This suggests that the risks and potential damage from flooding are increasing when considering both types of floods together.

Concerning the flood extent, the inundation area will cause damage to land use area. Potential land use damages are also analyzed against the simulated flood extents shown in Fig. 14. The most affected land cover type is pond, followed by settlement, industrial, farm, vacant land, river, and kaleyard. Furthermore, the exposure of the mentioned land use increases linearly concerning the flood event.

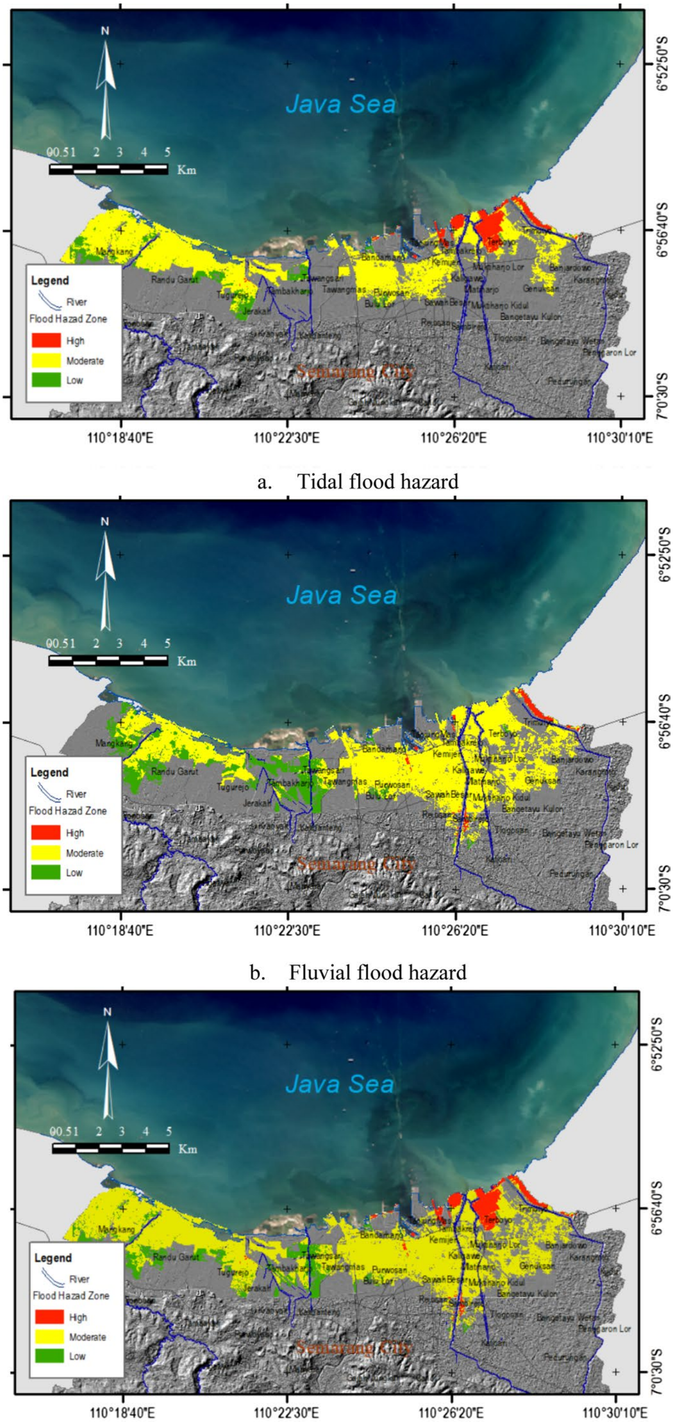

a. Tidal flood hazard

b. Fluvial flood hazard

c. Combined flood hazard

Fig. 13 Flood hazard zone in 50-year return period **a** Tidal **b** Fluvial **c** Combined Flood

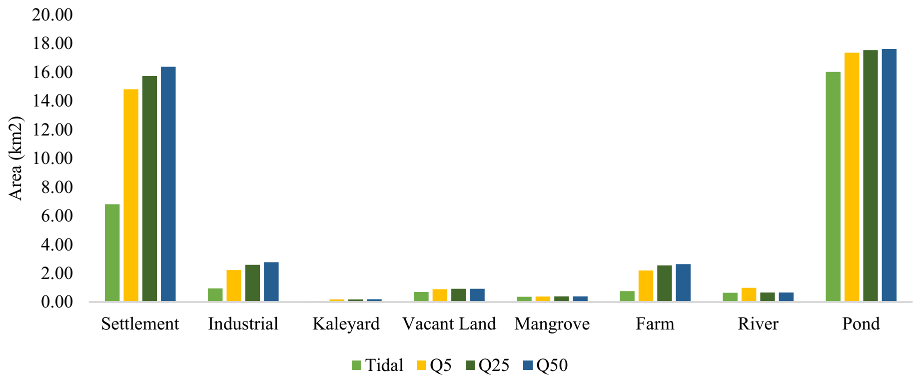

Fig. 14 Potential land use damages against tidal and flood recurrence events

5 Discussion

In terms of calibration and validation of the model, the result would be more accurate if it was calibrated and validated based on actual flood events (e.g., upstream and downstream flow hydrographs, mapped and documented inundation extents, depths, or flow velocities). Unfortunately, such data are difficult to find. Therefore, we employ field survey data and satellite image data. Regarding input data, the DEM is crucial in ensuring model accuracy. This paper attempts to assess flood inundation model sensitivity to different DEMs, namely DEMNAS, TerraSAR, and LiDAR under 50-year return period designed flood. The assessment shows that LiDAR is more sensitive. LiDAR DEM with a resolution of 1 m enables the creation of high-quality rasters for flow velocity and depth compared to DEMNAS and TerraSAR. LiDAR provides detailed and high-resolution elevation data, which are crucial for accurately representing the terrain and surface features in flood-prone areas.

In this study, the accuracy of the flood inundation modelling results is improved by river geometry data during the process of hydro-enforcement. In addition, since the condition of the surface topography in the study area is dynamic due to land subsidence, the DEM used for flood modelling is corrected using land subsidence rate. Land subsidence modelling using DinSAR is a quick assessment method that offers the advantage of mapping relatively large areas. However, it also comes with certain limitations. One of these limitations is its sensitivity to variations in environmental conditions, which can affect accuracy. From the results in **4.2**, flooding behavior indicates that the contribution of fluvial floods should not be ignored, even in water catchment areas where overflow floods are the main cause of flooding damage. Fluvial floods also make a significant contribution to urban floods, e.g., Kemijen, Mlatiharjo, Muktiharjo, and Genuksari. The significant depth and extensive coverage of this fluvial flood make it necessary to be cautious, especially for floodplain areas along major rivers such as the Kanal Timur, Tenggang, and Babon floods. On the other hand, tidal floods are characterized by higher flood depths, particularly in coastal regions adjacent to the sea, like Mangkang, Terboyo, and Trimulyo, which have topographic elevations lower than mean sea level (MSL). These coastal areas are more susceptible to the impact of tidal surges, leading to more severe flooding during tidal events.

The analysis results reveal a remarkably strong correlation between the rate of land subsidence and flood events. This correlation is particularly evident in the northern areas of Semarang City, such as Tambakharjo, Terboyo, and Genuksari, where the rate of land subsidence reaches more than 9 cm year[1], leading to flooding events with inundation depths more than 0.5 m. To determine categories of flood hazard levels, we conduct the process based on flood intensity and land subsidence which results in three categories: low, moderate, and high. Despite the different methodological basis, a similar pattern was also presented in another study conducted by BPBD (2022). It used fuzzy logic estimation based on slope and distance from river, which mentioned the high level is found in the northern part of Semarang's coastal area, e.g., Mangkang, Bandarharjo, Tawangmas Mlatiharjo, Kaligawe, and Gayamsari in the middle part Semarang.

Previous research proposed flood hazard levels based on depth and flow velocity (Kourgialas & Karatzas 2011). According to Vojtek and Vojteková (2016) defining flood hazard levels will depend on the impact of flood events and the characteristics of study areas. Baldassarre et al. (2009) proposed five levels of hazard following the USBR ACER Technical Memorandum No. 11 (1988). However, to determine categories of flood hazard levels, we conduct the process based on flood intensity and land subsidence which results in three categories: low, moderate, and high. Utilizing this categorization may provide more rigorous insight into the underlying uncertainties contained in future flood hazards, especially among "sinking" coastal cities around Indonesia or even the world.

In this paper, we have mapped flood-prone areas with a more detailed hazard level, taking into account flood intensity and the rate of land subsidence. Therefore, this paper can be studied further to analyze potential damage caused by floods. However, analyzing potential damage accurately requires more data processing (Budiyono et al. 2015). This study can also be developed further to evaluate indirect flood impacts. Related studied have been done such as (Hammond et al. 2013; Mehvar et al. 2018; Mahya et al. 2021).

6 Conclusions

To conclude, water bodies (mostly maritime wetlands and ponds) should be considered the most flood-prone areas, followed closely by settlements. It is important to mention that the Genuk district falls in the high-level hazard category for both fluvial and tidal flood scenarios. However, moderate hazard is also found in parts of the Tugu and Semarang Barat districts. This paper presents a hydrodynamic-based analysis that hopefully could give deeper insight into future flood adaptation and mitigation efforts.

Land subsidence, DEM, and flood depth are interconnected factors influencing flood vulnerability in an area. Areas with low elevations below sea level (as indicated by the DEM) are more prone to land subsidence, which exacerbates flooding by raising the relative sea level during inundation. Consequently, higher land subsidence rates lead to greater decreases in elevation over time, resulting in deeper flood depths during inundation events.

To complement the effort of Semarang coastal area flood risk reduction, strengthening the effort of reducing land subsidence, which is argued to contribute to 6.8% of flooding extension in Semarang (Irawan et al. 2021), is also essential. According to (Abidin et al.

2022) several programs proposed land subsidence risk reduction, i.e., improvement of the subsidence monitoring system and its governance, the realization of zero groundwater policy, strengthening subsidence-adaptive urban development, and strengthening land subsidence risk governance. On the other hand, mitigation of land subsidence can be done if the causes are known. So far, the investigation into the causes of land subsidence in Semarang is still being carried out, so the mitigation itself is indeed still below the best expectation so far (Andreas et al. 2017). Thus, we also encourage undergoing strategies proposed by the Coordinating Ministry for Maritime Affairs (2019) named "Coastal Land Subsidence Mitigation and Adaptation Road Map" to further study the groundwater basin's characteristics across Semarang as well as how to monitor them, so that the sustainability of groundwater and the healthy balance of "water supply versus demand" could be better planned, maintained, and regulated.

It was proven that assessment of flood risk induced by tidal and fluvial flood can be a useful tool for mapping flood extent, especially in the coastal area, i.e., which area experiences in land subsidence and tidal flooding monitoring. The study result can also be applied to the prevention of susceptible areas and flood risk management. Dissemination of flood risk and increasing public awareness of flood hazard should be proposed as the primary goals. Flood hazard level map can be used as reference in spatial planning, such as regulation in building expansion and density contraction in area with high-level flood hazard.

Ultimately, more detailed studies on a finer scale regarding moderate–high hazard areas that incorporate more detailed technical considerations such as existing water infrastructure are encouraged to better depict what best solution fits for respected study areas. We also encourage further study by incorporating analysis, not only on a hazard but also vulnerability and capacity rate in the face of flood disaster, to fully understand the flood risk circumstances in Semarang whether stochastic-based or analytical-based.

Appendix 1: Flow accumulation from different DEMs

Flow accumulation is an important factor in understanding and forecasting flood-prone locations. It is the amount of flow that builds in each raster pixel based on the cumulative weights of the pixels before it (Negese et al. 2022). Researchers can identify flood-prone places by examining flow accumulation patterns (Yunus 2021; Negese et al. 2022).

As shown in Fig. 15 and Table 10 the flow accumulation determined from different DEM resolutions statistically shows that when the resolution goes from fine to coarse, the maximum, mean, and standard deviation flow accumulations drop dramatically. When the DEM resolution is reduced from 1 to 9 m, from LiDAR to TerraSAR, the mean flow accumulation is reduced by one-third, while the maximum and standard deviation of flow accumulation are reduced by one-fourth.

A high DEM resolution enables the collection of more values. In other words, the greater the value of max flow accumulation, the greater the number of rivers or water bodies derived from the DEM, and the greater the potential of inundation area as related to flood extent findings as mentioned in Table 5. A more accurate representation of

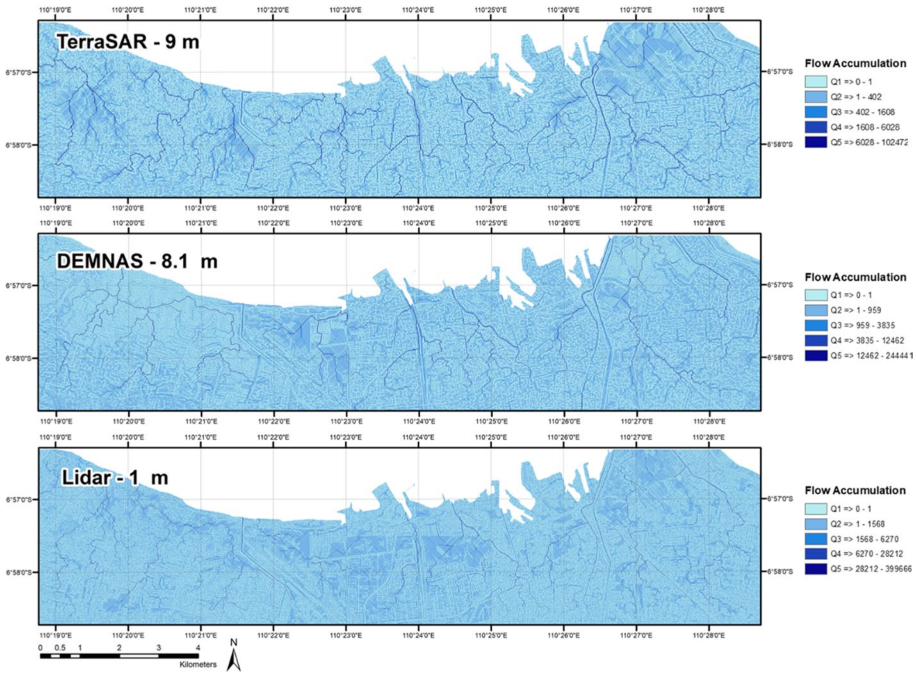

Fig. 15 Flow accumulation value and distribution differences Between TerraSAR, DEMNAS, and LiDAR DEM

Table 10 Flow accumulation statistics of different DEMs tested in this study (TerraSAR, DEMNAS, and LiDAR)

Statistic	Flow accumulation/m^2		
	TerraSAR—9 m	DEMNAS—8.1 m	LiDAR—1 m
Mean	192	328	536
Max	102,472	244,441	399,666
Standard deviation	2186	4793	8532

complicated topography will be possible with smaller grid cell sizes, and thus, high-resolution DEMs are better equipped to refine complex topographic characteristics (Wechsler 2006). If the topography is complex, larger differences between grid cells can be predicted. The surface would appear very varied over short distances, but observed slopes would be relatively consistent regardless of where they were tested over longer distances (Warren et al. 2004).

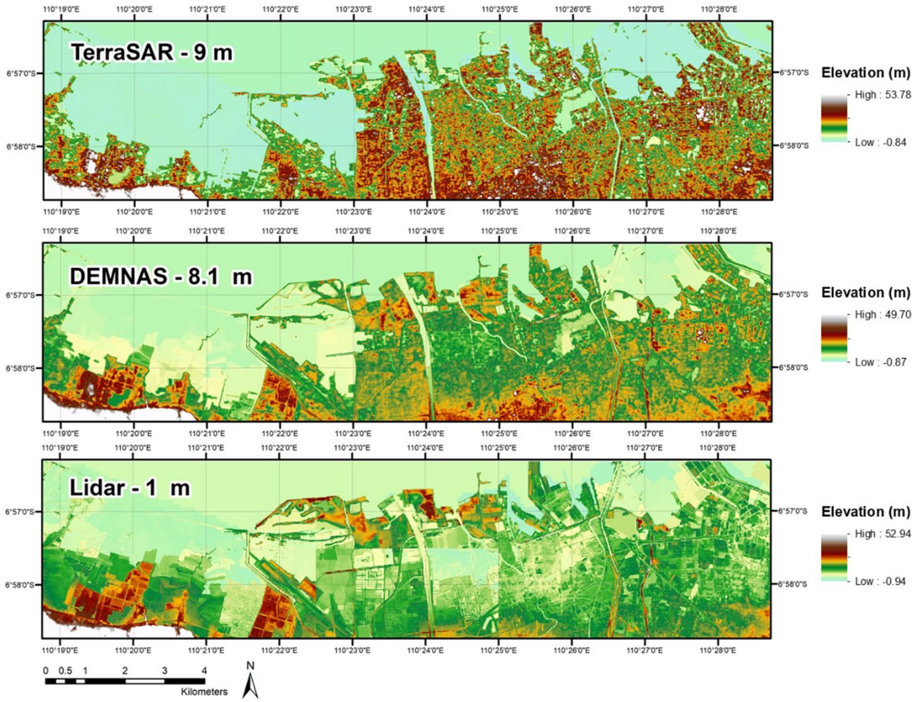

Fig. 16 Elevation values and distribution differences between TerraSAR, DEMNAS, and LiDAR DEM

This explains how the slope becomes comparable or a smoothing effect develops in the observed slopes at low DEM resolutions. As a result, most low DEM resolution values are smoothed according to the major flow accumulation value, resulting in a drop in flow accumulation mean and standard deviation concerning its limited measured slope variability. This consideration is highly relevant to the visualized digital elevation model depicted in Fig. 16, where the topography is becoming very complex in the LiDAR DEM with clearly-bordered boxy pattern relevant to the Semarang's urban coastal landscape, thus resulting in higher accuracy of modelled flood extent and depth, as opposed to the smoothed elevation differences found in DEMNAS and TerraSAR that produce a less satisfying result.

Acknowledgements This research is funded by BUDI DN Doctoral Scholarship from the Lembaga Pengelola Dana Penelitian (LPDP), Ministry of Finance and Ministry of Research, Technology and Higher Education, Republic of Indonesia, and Research Doctoral Dissertation grand number FITB.PN-1-03-2021 from Ministry of Research and Technology/BRIN.

Author contributions "All authors contributed to the study conception and design. Material preparation, data collection, and analysis were performed by BDY, HZA, P, HA, ASPP, and FG. The first draft of the manuscript was written by BDY, and all authors commented on previous versions of the manuscript. All authors read and approved the final manuscript."

Funding The authors have not disclosed any funding.

Declarations

Conflict of interest The authors have no relevant financial or non-financial interests to disclose.

Ethical approval Hereby, I, Bambang Darmo Yuwono, consciously assure that for the manuscript Mapping of flood hazard induced by land subsidence in Semarang City, Indonesia, using hydraulic and spatial models, the following is fulfilled: (1) This material is the author's own original work, which has not been previously published elsewhere. (2) The paper is not currently being considered for publication elsewhere. (3) The paper reflects the authors' own research and analysis in a truthful and complete manner. (4) The paper properly credits the meaningful contributions of co-authors and co-researchers. (5) The results are appropriately placed in the context of prior and existing research. (6) All sources used are properly disclosed (correct citation). Literally copying of text must be indicated as such by using quotation marks and giving proper reference. (7) All authors have been personally and actively involved in substantial work leading to the paper and will take public responsibility for its content.

References

Abidin HZ, Andreas H, Gumilar I, et al (2010) Studying land subsidence in Semarang (indonesia) using geodetic methods. FIG Congr 11–16. https://www.fig.net/resources/proceedings/fig_proceedings/fig2010/papers/fs04d/fs04d_abidin_andreas_et_al_3748.pdf

Abidin HZ, Andreas H, Gumilar I, Fukuda Y, Nurmaulia SL, Riawan E, Murdohardono D, Supriyadi (2012) The impacts of coastal subsidence and sea level rise in coastal city of Semarang (Indonesia). Adv Geosci: Solid Earth Sci 31:59–75

Abidin HZ et al (2013) Land subsidence in coastal city of Semarang (Indonesia): characteristics, impacts and causes. Geomat, Nat Hazards Risk 4(3):226–240. https://doi.org/10.1080/19475705.2012.692336

Abidin H et al (2015) On integration of geodetic observation of land subsidence hazard risk in urban area of Indonesia. Int as Geod Symp. https://doi.org/10.1007/1345

Abidin HZ, Andreas H, Gumilar I et al (2022) On the Disaster Risk Reduction of Land Subsidence in Indonesia's Northern Coastal Areas of Java. EGU Gen Assem 5194:EGU22–1721. https://meetingorganizer.copernicus.org/EGU22/EGU22-1721.html

Aini NI, Filjanah Q (2020) Pola Pengendalian Banjir pada Sungai Tenggang Kecamatan Genuk Kota Semarang Dengan Menggunakan Metode Hec-Ras. 5:96–103.

Aldridge BN, Garrett JM (1973) Roughness coefficients for stream channels in Arizona: U.S. geological survey open-file report. 87

Amar M et al (2020) Analisis geospasial korelasi penurunan muka tanah terhadap harga tanah di wilayah kecamatan Semarang utara. J Geod Undip 9(2):63–70

Andnur MO et al (2022) Analisis tinggi muka air laut dan penurunan muka tanah untuk perencanaan tinggi lantai bangunan di Pesisir Utara Kota Semarang. Indones J Oceanogr (IJOCE) 04(02):56–60

Andreas H et al (2017) Adaptation and mitigation of land subsidence in Semarang. AIP Conf Proc. https://doi.org/10.1063/1.4987088

Andreas H, Abidin HZ, Gumilar I, Sidiq TP, Sarsito DA, Pradipta D (2019) On the acceleration of land subsidence rate in Semarang City as detected from GPS surveys, E3S Web of Conferences. In: Proceedings of the international symposium on global navigation satellite sys-tem 2018 (ISGNSS 2018), Bali, 94, 21–23 Nov. 2018, doi: https://doi.org/10.1051/e3sconf/20199404002

Apel H, Aronica GT, Kreibich H, Thieken AH (2009) Flood risk analyses—how detailed do we need to be? Nat Hazards 49(1):79–98

Arcement G J, Schneider V R (1989) Guide for selecting manning's roughness coefficients for natural channels and flood plains. 2339

Atriyon J, Djurdjani (2018) Journal of degraded and mining lands management Azotobacter population, soil nitrogen and groundnut growth in mercury-contaminated tailing inoculated with Azotobacter. J Degrade Min Land Manag 5(53):2502–2458. https://doi.org/10.15243/jdmlm

Balai Pengelolaan DAS (BPDAS) (2015) Report on monitoring and evaluation of cacaban watershed management 2015. Semarang: BPDAS Pemali Jratun

Brunner GW, Piper SS, Jensen MR, Chacon B (2015) Combined 1D and 2D hydraulic modelling within HEC-RAS. World Environ Water Resour Congr 2015:1432–1443

Brunner GW (2016) HEC-RAS river analysis system: Hydraulic Reference Manual, Version 5.0. US Army Corps of Engineers, Institute for Water Resources, Hydrologic Engineering

Budiyono Y et al (2015) Flood risk assessment for delta mega-cities: a case study of Jakarta. Nat Hazards 75(1):389–413. https://doi.org/10.1007/s11069-014-1327-9

Chaussard E, Amelung F, Abidin H, Hong SH (2013) Sinking cities in Indonesia: ALOS PALSAR detects rapid subsidence due to groundwater and gas extraction. Remote Sens Environ 128:150–161. https://doi.org/10.1016/j.rse.2012.10.015

Chow VT (1959) Open-channel hydraulics. New York (NY): McGraw-Hill Higher Education

Dasallas L, Kim Y, An H (2019) Case study of HEC-RAS 1D–2D coupling simulation: 2002 Baeksan flood event in Korea. Water 11(10):2048

Dewi A (2007) Community-based analysis of coping with urban flooding: a case study in Semarang, Indonesia. International Institute for Geo-Information Science and Earth Observation Enschede, The Netherlands, p 79

Di Baldassarre G, Montanari A (2009) Uncertainty in river discharge observations: a quantitative analysis. Hydrol Earth Syst Sci 13(6):913–921. https://doi.org/10.5194/hess-13-913-2009

Drbal K, Stepankova P, Levitus V, Rıha J, Drab A, Satrapa L, Horsky M, Valenta P, alentova J, Friedmannova L (2009) Metodika tvorby map povodnoveho nebezpecı a povodnovych rizik [Methodology for creating maps offlood hazard and flood risk]. Brno: VUV TGM.

Hammond MJ et al (2013) A framework for flood impact assessment in urban areas. IAHS AISH Publ 357(January):41–47

Han D, Hu Z, Yang M, Wang Y, Chen L, Gao Y (2020) Assessing the impacts of DEM resolution on flood hazard mapping. Water 12(10):2856. https://doi.org/10.3390/w12102856

Handoyo G et al (2016) Genangan banjir rob Di Kecamatan Semarang Utara. J Kelaut Trop 19(1):55. https://doi.org/10.14710/jkt.v19i1.601

Van de Haterd J et al (2021) Environmental change and health risks in coastal Semarang, Indonesia: importance of local indigenous knowledge for strengthening adaptation policies. Cit Health 5(3):276–288. https://doi.org/10.1080/23748834.2020.1729451

Horritt MS, Bates PD (2001) Predicting floodplain inundation: raster-based modelling versus the finite-element approach. Hydrol Process 15(5):825–842. https://doi.org/10.1002/hyp.188

Horritt MS, Bates PD (2002) Evaluation of 1D and 2D numerical models for predicting river flood inundation. J Hydrol 64:628–638. https://doi.org/10.1016/S0022-1694(02)00121-X

Horritt MS, Di Baldassarre G, Bates PD, Brath A (2007) Comparing the performance of a 2-D finite element and a 2-D finite volume model of floodplain inundation using airborne SAR imagery. Hydrol Process: Int J 21(20):2745–2759

Irawan AM, Marfai MA, Nugraheni IR, et al (2021) Comparison between averaged and localised subsidence measurements for coastal floods projection in 2050 Semarang, Indonesia. Urban Clim 35:100760. https://doi.org/10.1016/j.uclim.2020.100760

Ismanto A et al (2012) Model sebaran penurunan tanah di wilayah pesisir Semarang. Ilmu Kelautan—Indones J Mar Sci 14(4):189–196

Istiqomah LN et al (2020) Analisis penurunan muka tanah Kota Semarang metode survei GNSS tahun 2019. J Geod Undip 4(April):86–94

Khattak MS et al (2016) Floodplain mapping Using HEC-RAS and ArcGIS: a case study of Kabul River. Arab J Sci Eng 41(4):1375–1390. https://doi.org/10.1007/s13369-015-1915-3

Kobayashi H (2003) Vulnerability assessment and adaptation strategy to sea-level rise in Indonesian coastal urban areas. Asahi-1, Tsukuba-city, Japan: National institute for land and infrastructure management, ministry of land, infrastructure and transport

Kourgialas NN, Karatzas GP (2011) Gestion des inondations et méthode de modélisation sous SIG pour évaluer les zones d'aléa inondation-une étude de cas. Hydrol Sci J 56(2):212–225. https://doi.org/10.1080/02626667.2011.555836

Kuehn F et al (2010) Detection of land subsidence in Semarang, Indonesia, using stable points network (SPN) technique. Environ Earth Sci 60(5):909–921. https://doi.org/10.1007/s12665-009-0227-x

Kurniawati W et al (2020) Spatial Expression of Malay Kampung Semarang in facing flood disaster. IOP Conf Ser: Earth Environ Sci 409(1):012049. https://doi.org/10.1088/1755-1315/409/1/012049

Liu Y, Huang H, Dong J (2015) Large-area land subsidence monitoring and mechanism research using the small baseline subset interferometric synthetic aperture radar technique over the Yellow River Delta, China. J Appl Remote Sens 9:096019–096019. https://doi.org/10.1117/1.JRS.9.096019

Liu Z, Merwade V, Jafarzadegan K (2019) Investigating the role of model structure and surface roughness in generating flood inundation extents using one-and two-dimensional hydraulic models. J Flood Risk Manag 12(1):e12347

Lubis AM, Sato T, Tomiyama N, Isezaki N, Yamanokuchi T (2011) Ground subsidence in Semarang-Indonesia investigated by ALOS-PALSAR satellite SAR interferometry. J Asian Earth Sci 40:1079–1088. https://doi.org/10.1016/j.jseaes.2010.12.001

Luo Q, Perissin D, Zhang Y, Jia Y (2014) L- and X-band multi- temporal InSAR analysis of tianjin subsidence. Remote Sens 6:7933–7951. https://doi.org/10.3390/rs6097933

Mahya M, Kok S, Cado van der Leij A (2021) Economic assessment of subsidence in Semarang and Demak, Indonesia. 61. https://www.ecoshape.org/app/uploads/sites/2/2017/08/Economic-assessment-of-subsidence-in-Semarang-and-Demak-Indonesia.pdf

Mason DC et al (2010) Flood detection in Urban areas using TerraSAR-X. IEEE Trans Geosci Remote Sens 48(2):882–894. https://doi.org/10.1109/TGRS.2009.2029236

Marfai MA (2014) Impact of sea level rise to coastal ecology: a case study on the northern part of java island, indonesia. Quaest Geogr 33(1):107–114. https://doi.org/10.2478/quageo-2014-0008

Marfai MA et al (2008) The impact of tidal flooding on a coastal community in Semarang, Indonesia. Environmentalist 28(3):237–248. https://doi.org/10.1007/s10669-007-9134-4

Marfai MA, King L (2008) Tidal inundation mapping under enhanced land subsidence in Semarang, Central Java Indonesia. Nat Hazards 44(1):93–109. https://doi.org/10.1007/s11069-007-9144-z

Marfai MA, King L (2007) Monitoring land subsidence in Semarang, Indonesia. Environ Geol 53(3):651–659. https://doi.org/10.1007/s00254-007-0680-3

McInnes KL et al (2003) Impact of sea-level rise and storm surges in a coastal community. Nat Hazards 30(2):187–207. https://doi.org/10.1023/A:1026118417752

Martins R, Leandro J, Chen AS, Djordjević S (2017) A comparison of three dual drainage models: shallow water versus local inertial vs. Diffus Wave J Hydroinform 19:331–348

Mehvar S et al (2018) Developing a framework to quantify potential Sea level rise-driven environmental losses: a case study in Semarang coastal area, Indonesia. Environ Sci Policy 89(February):216–230. https://doi.org/10.1016/j.envsci.2018.06.019

Merz B et al (2010) Review article assessment of economic flood damage. Nat Hazards Earth Syst Sci 10(8):1697–1724. https://doi.org/10.5194/nhess-10-1697-2010

Moore ID et al (1991) Digital terrain modelling: a review of hydrological, geomorphological, and biological applications. Hydrol Process 5(1):3–30. https://doi.org/10.1002/hyp.3360050103

Murdohardono D, Tobing TMHL, Sayekti A (2007) Over Pumping ff Ground Water as one of Causes of Sea Water Inundation in Semarang City, Paper presented at the International Symposium and Workshop on Current Ptidal floodinflems in Groundwater Management and Related Water Reosurces Issues, Kuta, Bali, 3-8 December 2007

National Agency for Disaster Management; Badan Nasional Penanggulan Bencana, Agency: BNPB (2016) 'Resiko Bencana Indonesia'. https://bnpb.go.id/storage/app/media//uploads/24/buku-rbi-1.pdf

Negese A, Ayalew D, Shitaye A, Getnet H (2022) Potential flood-prone area identification and mapping using gis-based multi-criteria decision-making and analytical hierarchy process in Dega Damot District Northwestern Ethiopia. Appl Water Sci 12(12):255. https://doi.org/10.1007/s13201-022-01772-7

Prasetyo Y et al (2013) Data optimalization in permanent scatterer interferometric synthetic aperture radar (PS-INSAR) technique for land subsidence estimation. In: 34th asian conference on remote sensing 2013, ACRS 2013, 2, pp 1064–1072

Prasetyo Y et al (2018) Spatial analysis of land subsidence and flood pattern based on DInSAR method in sentinel sar imagery and weighting method in geo-hazard parameters combination in North Jakarta Region. IOP Conf Ser: Earth Environ Sci. https://doi.org/10.1088/1755-1315/123/1/012009

Pratikno N, Handayani W (2014) Pengaruh genangan banjir rob terhadap dinamika sosial ekonomi masyarakat kelurahan Bandarharjo, Semarang. Tek PWK (perencanaan Wilayah Kota) 3(2):312–318

Pujiastuti R et al (2016) Pengaruh land subsidence terhadap genangan banjir dan rob di Semarang timur. Med Komun Tek Sipil 21(1):1. https://doi.org/10.14710/mkts.v21i1.11225

Putra ISW et al (2020) Penilaian kerusakan dan kerugian infrastruktur publik akibat dampak bencana banjir Di Kota Semarang. Wahana Tek Sipil: J Pengemb Tek Sipil 25(2):86. https://doi.org/10.32497/wahanats.v25i2.2154

Qi H, Altinakar MS (2011) A GIS-based decision support system for integrated flood management under uncertainty with two dimensional numerical simulations. Environ Model Softw 26(6):817–821. https://doi.org/10.1016/j.envsoft.2010.11.006

Qin Z, Qin C, Zhang J, Huang Q, Zhang Y, Huang Y (2018) Sensitivity of flood simulation to DEM resolution, spatial rainfall resolution, and flow direction algorithm in SWAT. Water 10(7):887. https://doi.org/10.3390/w10070887

Quiroga VM, Kurea S, Udoa K, Manoa A (2016) Application of 2D numerical simulation for the analysis of the February 2014 Bolivian Amazonia flood: application of the new HEC-RAS version 5. Ribagua 3(1):25–33

Razali N, Ismail S, Mustapha A (2020) Machine learning approach for flood risks prediction. IAES Int J Artif Intell 9:73–80. https://doi.org/10.11591/ijai.v9.i1

Regional Agency for Disaster Management: Badan Penanggulangan Bencana Daerah: (BPBD), Semarang City (2022). https://semarisk.bpbd.semarangkota.go.id/download/1_PETA%20ANCAMAN%20BANJIR.pdf

Setioko B et al (2013) Towards sustainable urban growth: the unaffected fisherman settlement setting (with case study Semarang coastal area). Procedia Environ Sci 17:401–407. https://doi.org/10.1016/j.proenv.2013.02.053
Srivastava A, Tiwari A, Narayan AB, Dikshit O (2022) InSAR phase unwrapping using Graph neural networks, EGU General Assembly 2022, Vienna, Austria, 23–27 May 2022, EGU22-11010, https://doi.org/10.5194/egusphere-egu22-11010
Suhelmi IR et al (2014) Potential economic losses due to tidal inundation and flood at Semarang City. Forum Geografi 28(2):113–118. https://doi.org/10.23917/forgeo.v28i2.428
Supriyadi (2008). Separation of gravity anomaly caused subsidence and ground water level lowering of time lapse microgravity data using model based filter: case study Semarang aluvial plain (in Indonesian), PhD Dissertation. Institute of Technology Bandung, September, 146 pp
Tarekegn TH et al (2010) Assessment of an ASTER-generated DEM for 2D hydrodynamic flood modeling. Int J Appl Earth Obs Geoinf 12(6):457–465. https://doi.org/10.1016/j.jag.2010.05.007
Uddin K, Matin MA (2021) Potential flood hazard zonation and flood shelter suitability mapping for disaster risk mitigation in Bangladesh using geospatial technology. Prog Disaster Sci 11:100185. https://doi.org/10.1016/j.pdisas.2021.100185
Utami I, Marzuki M (2020) Analisis sistem informasi banjir berbasis media twitter. J Fis Unand 9(1):67–72
Vojtek M, Vojteková J (2016) Flood hazard and flood risk assessment at the local spatial scale: a case study. Geomat Nat Hazards Risk 7(6):1973–1992. https://doi.org/10.1080/19475705.2016.1166874
Ward PJ, Marfai MA, Yulianto F, et al (2011) Coastal inundation and damage exposure estimation: a case study for Jakarta. Nat Hazards 56:899–916. https://doi.org/10.1007/s11069-010-9599-1
Warren SD, Hohmann MG, Auerswald K, Mitasova H (2004) An evaluation of methods to determine slope using digital elevation data. CATENA 58:215–233. https://doi.org/10.1016/j.catena.2004.05.001
Waskitaningsih N (2012) Kearifan lokal masyarakat sub-sistem drainase bringin dalam menghadapi banjir. J Pembang Wil Kota 8(4):383. https://doi.org/10.14710/pwk.v8i4.6495
Wechsler SP (2006) Uncertainties associated with digital elevation models for hydrologic applications: a review. Hydrol Earth Syst Sci Discuss 3:2343–2384. https://doi.org/10.5194/hessd-3-2343-2006
Wedajo GK (2017) LiDAR DEM data for flood mapping and assessment; opportunities and challenges: a review. J Remote Sens GIS 06:2015–2018. https://doi.org/10.4172/2469-4134.1000211
Wirawan AR et al (2019) Pengamatan penurunan muka tanah Kota Semarang metode survei GNSS Tahun 2018. J Geod Undip 8(1):418–427
Wismarini TD, Ningsih DHU (2010) Analisis sistem drainase Kota Semarang berbasis sistem informasi geografi dalam membantu pengambilan keputusan bagi penanganan banjir. J Teknol Inf DINAMIK 15(1):41–51
Xu K, Fang J, Fang Y, et al (2021) The importance of digital elevation model selection in flood simulation and a proposed method to reduce dem errors: a case study in shanghai. Int J Disaster Risk Sci 12:890–902. https://doi.org/10.1007/s13753-021-00377-z
Yastika PE et al (2019) Monitoring of long-term land subsidence from 2003 to 2017 in coastal area of Semarang, Indonesia by SBAS DInSAR analyses using Envisat-ASAR, ALOS-PALSAR, and Sentinel-1A SAR data. Adv Space Res 63(5):1719–1736. https://doi.org/10.1016/j.asr.2018.11.008
Yunus S (2021) Delineation of urban flood risk areas using geospatial technique. Fudma J Sci 1(5):1–10
Yuwono BD et al (2016) Preliminary survey and performance of land subsidence in North Semarang Demak. AIP Conf Proc 1730(May):1–12. https://doi.org/10.1063/1.4947410
Yuwono BD et al (2019) Land subsidence monitoring 2016–2018 analysis using GNSS CORS UDIP and DinSAR in Semarang. KnE Eng 2019:95–105. https://doi.org/10.18502/keg.v4i3.5832
Zainuri M et al (2022) An improve performance of geospatial model to access the tidal flood impact on land use by evaluating sea level rise and land subsidence parameters. J Ecol Eng 23(2):1–11. https://doi.org/10.12911/22998993/144785